(12) LEVEL II

DNA 5209F

DESIGN AND DEVELOPMENT OF A HYDROFRAC STEAM GENERATOR SYSTEM

P. L. Lagus
D. D. Ellefson
P. L. Turner

Systems, Science and Software
P.O. Box 1620
La Jolla, California 92038

1 January 1980

Final Report for Period 15 May 1978—1 January 1980

CONTRACT No. DNA 001-78-C-0262

APPROVED FOR PUBLIC RELEASE;
DISTRIBUTION UNLIMITED.

THIS WORK SPONSORED BY THE DEFENSE NUCLEAR AGENCY
UNDER RDT&E RMSS CODE B345078462 J24AAXYX98357 H2590D.

Prepared for
Director
DEFENSE NUCLEAR AGENCY
Washington, D. C. 20305

Destroy this report when it is no longer needed. Do not return to sender.

PLEASE NOTIFY THE DEFENSE NUCLEAR AGENCY, ATTN: STTI, WASHINGTON, D.C. 20305, IF YOUR ADDRESS IS INCORRECT, IF YOU WISH TO BE DELETED FROM THE DISTRIBUTION LIST, OR IF THE ADDRESSEE IS NO LONGER EMPLOYED BY YOUR ORGANIZATION.

18 DNA, SBIE

UNCLASSIFIED

SECURITY CLASSIFICATION OF THIS PAGE (When Data Entered)

REPORT DOCUMENTATION PAGE	READ INSTRUCTIONS BEFORE COMPLETING FORM
1. REPORT NUMBER: DNA 5209F AD-E300 194	2. GOVT ACCESSION NO. AD-A088913	3. RECIPIENT'S CATALOG NUMBER
4. TITLE (and Subtitle): DESIGN AND DEVELOPMENT OF A HYDROFRAC STEAM GENERATOR SYSTEM.	5. TYPE OF REPORT & PERIOD COVERED: FINAL REPORT. 15 May 78 — 1 Jan 80
	6. PERFORMING ORG. REPORT NUMBER: SSS-R-80-4347
7. AUTHOR(s): Peter L. Lagus, Larry D. Ellefson, Phil Turner	8. CONTRACT OR GRANT NUMBER(s): DNA 001-78-C-0262
9. PERFORMING ORGANIZATION NAME AND ADDRESS: Systems, Science and Software, P.O. Box 1620, La Jolla, CA 92038	10. PROGRAM ELEMENT, PROJECT, TASK AREA & WORK UNIT NUMBERS: SUBTASK J24AAXYX98357
11. CONTROLLING OFFICE NAME AND ADDRESS: Director, Defense Nuclear Agency, Washington, D.C. 20305	12. REPORT DATE: 1 Jan 80
	13. NUMBER OF PAGES: 90
14. MONITORING AGENCY NAME & ADDRESS (if different from Controlling Office)	15. SECURITY CLASS (of this report): Unclassified
	15a. DECLASSIFICATION DOWNGRADING SCHEDULE

16. DISTRIBUTION STATEMENT (of this Report)

Approved for public release; distribution unlimited.

17. DISTRIBUTION STATEMENT (of the abstract entered in Block 20, if different from Report)

18. SUPPLEMENTARY NOTES

This work sponsored by the Defense Nuclear Agency under RDT&E RMSS Code B345078462 J24AAXYX98357 H2590D.

19. KEY WORDS (Continue on reverse side if necessary and identify by block number)

Hydrogen-oxygen combustion

Steam hydrofrac

20. ABSTRACT (Continue on reverse side if necessary and identify by block number)

A controllable steam generator utilizing hydrogen, oxygen and water has been developed. Steam possessing a wide range of thermodynamic conditions can be produced with this generator. Ultimate production is 30 moles of steam per second at pressures of 10 MPa and temperatures of roughly 700°C. Preliminary testing was conducted in a high-pressure test chamber. These tests demonstrate the ability of the generator to produce

→over

DD FORM 1 JAN 73 1473 EDITION OF 1 NOV 65 IS OBSOLETE

UNCLASSIFIED

SECURITY CLASSIFICATION OF THIS PAGE (When Data Entered)

388507

copious quantities of steam in a controlled fashion. On the basis of this work it appears that it is possible to configure the generator as a drill hole probe.

TABLE OF CONTENTS

SECTION		PAGE
	LIST OF ILLUSTRATIONS	2
	LIST OF TABLES	5
I.	INTRODUCTION	7
II.	TECHNICAL DISCUSSION	9
III.	EQUIPMENT DESIGN	13
	PRESSURE/COMBUSTION CHAMBER	13
	TORCH HEAD	17
	IGNITION SYSTEM	25
	WATER INJECTION	25
	GAS SUPPLY	31
	ELECTRICAL EQUIPMENT DESIGN	31
IV.	INSTRUMENTATION AND CONTROLS	33
	PRESSURE REGULATION FOR H_2 AND O_2	33
	FLOWRATE CONTROL FOR H_2 AND O_2	33
	PRESSURE AND TEMPERATURE MONITORING	40
V.	PROCESS CONTROL	47
	SIZING OF THE STEAM EXIT ORIFICE	47
	FLOW ANALYSIS OF H_2 AND O_2	52
	FLOW ANALYSIS OF THE WATER	60
VI.	DATA AND RESULTS	63
	EXPERIMENT I	64
	EXPERIMENT II	70
	APPENDIX A - CALCULATION OF THE ADIABATIC FLAME TEMPERATURE	75
	APPENDIX B - CALIBRATION OF FLOW CONTROL VALVES	77
	APPENDIX C - SPECIFICATIONS FOR THE THERMAL INSULATION	83
	APPENDIX D - SAFETY AND SYSTEM CHECK OUT	85

LIST OF ILLUSTRATIONS

FIGURE		PAGE
1	Adiabatic, constant pressure flame temperature ($\Delta H \equiv 0$) for $2H_2 + O_2 + nH_2O(\ell) \rightarrow (n+2)\ H_2O$ ideal gas equation of state assumed.	11
2	Flow diagram for the H_2/O_2 Steam Generator.	14
3	Overall view of the test site.	15
4	Steam generator chamber, 8803 cm^3 chamber volume.	16
5	Overall view of chamber on test stand.	18
6	Test chamber (top view) showing ceramic insulation.	19
7	View of the bottom of the chamber.	20
8	Thermal insulation and protective liner.	21
9	Torch head modified to accommodate water flow.	22
10	Drawing of tip modified for external mixing.	24
11	Block diagram of the ignition system.	26
12	Controls for adjusting the water flow rate.	28
13	Water pump and pressure pulsation dampener.	29
14	Water spray pattern.	30
15	Control and recording module (close-up of controller).	34
16	First and second stage regulators and digitally controlled metering valves mounted on-line.	35
17	Close-up view of the stepping motor.	36
18	Drawing of the front panel of the controller.	38

LIST OF ILLUSTRATIONS (continued)

FIGURE		PAGE
19	Functional block diagram of the controller for digitally controlled valves.	41
20	Block diagram of the pressure and temperature monitoring and recording systems.	42
21	Block diagram of the dome regulators control system.	45
22	Process flow diagram.	47
23	Chamber pressure versus time.	48
24	Flowrate of steam versus time.	48
25	Typical flow diagram for hydrogen and oxygen.	52
26	Flowrate of H_2 versus time with P_1 at 11.14 MPa and a fixed valve setting.	54
27	Flowrate of O_2 versus time with P_1 at 11.14 MPa and a fixed valve setting.	54
28	Ramps for increasing flow of hydrogen and oxygen as the chamber pressure increases.	56
29	Conceptual illustration of the flowrates of H_2 and O_2 versus time.	57
30	Illustration of the law of conservation of mass.	58
31	Flow capacity curve for the water valve.	61
32	Strip chart recording of the chamber pressure and temperature.	68
33	Strip chart recording of chamber temperature and ΔP across water metering valve.	69
34	Strip chart recording of the chamber pressure and temperature.	73
35	Strip chart recording of the chamber temperature and ΔP across water valve.	74

LIST OF ILLUSTRATIONS (continued)

FIGURE		PAGE
B-1	Calibration of a valve.	77
B-2	Flow capacity curve for the H_2 valve.	79
B-3	Flow capacity curve for the O_2 valve.	80

LIST OF TABLES

TABLE		PAGE
B-1	TEST DATA FOR THE H_2 VALVE.	81
B-2	TEST DATA FOR THE O_2 VALVE.	82
C-1	PHYSICAL PROPERTIES OF THE THERMAL INSULATION.	83

I. INTRODUCTION

For several years hydrofracture has been recognized as a potential failure mechanism which may compromise the containment of underground nuclear explosions. Very little quantitative data exists about hydrofracture processes in the tuff of Area 12 (Nevada Test Site) and no data is available from a steam-driven hydrofrac. The latter is particularly unfortunate since steam is likely to be the medium of concern in any forthcoming test. In addition, the physical processes involved in a condensable medium hydrofrac are more complex than those associated with more conventional gas or liquid hydrofracture systems. For instance, condensable hydrofracture involves the coupled interaction of heat transfer, condensation, gas and liquid diffusion, viscous flow, and crack development phenomena. These various processes have been incorporated into a numerical model, KRAK, developed at the Los Alamos Scientific Laboratory.

The primary objective of this work was to design and develop a hydrogen/oxygen steam generator which would produce copious quantities of high pressure, high temperature superheated steam. Emphasis had to be placed on problems of using high pressure hydrogen and oxygen in a controllable and safe manner. A secondary objective was to understand the fundamental engineering problems and limitations which might be encountered in a full-scale effort to produce a borehole steam generating probe.

This report details work performed during the previous year under contract DNA 001-78-C-0262. Section II elaborates the physical principles underlying the hydrogen-oxygen steam generator. Section III discusses the equipment design. Section IV provides details of the instrumentation and controls. Section V discusses the process control. Section VI presents the results of two experiments in which high pressure , high temperature steam was produced.

In addition, four appendices are provided. In Appendix A, the derivation for the adiabatic flame temperature is presented; in Appendix B, the calibration methodology and the calibration curves for the hydrogen and oxygen flow control valves are presented. Appendix C lists the physical properties for the thermal insulation utilized in the torch test vessel. Appendix D discusses safety and system check out procedures.

II. TECHNICAL DISCUSSION

The objective of the previous year's work was to design, fabricate and test a prototype system utilizing hydrogen, oxygen and water for generating copious quantities of steam possessing known thermodynamic conditions. Quantitative data were obtained on the various flow parameters involved in the generation of the steam. In addition, the system was to be controllable to the point where one could alter the thermodynamic state of the steam from experiment to experiment. These considerations led us to consider a water cooled hydrogen and oxygen flame. Our initial reaction to the idea was negative because of the obvious safety concern associated with it. On the other hand, the fact that the gases are highly reactive is of major assistance in developing an overall system. The gas ignition and process control have turned out to be relatively straightforward.

The chemical reaction for a stoichiometric mixture of hydrogen and oxygen can be illustrated by the following chemical equation:

$$2\ H_2 + O_2 \rightarrow 2\ H_2O + \text{heat} \qquad (1)$$

This equation states that two moles of hydrogen react with one mole of oxygen to produce two moles of water (steam). This reaction is highly exothermic. Therefore, water (liquid) can be added to absorb this heat of combustion and produce additional quantities of steam. The injected water does not enter the chemical reaction but merely absorbs heat, thus lowering the adiabatic flame temperature. The adiabatic flame temperature is the temperature of the products of combustion assuming no heat transfer across the system boundary. Furthermore, the injection of water does not quench the flame because the combustion of hydrogen and oxygen is so highly reactive and exothermic. This reaction with the addition of water can be expressed as:

$$2\ H_2 + O_2 + n\ H_2O \rightarrow (n + 2)\ H_2O \qquad (2)$$

The flame temperature is controlled by the number of moles of water injected. With the addition of six moles (n=6) of water, the resulting adiabatic flame temperature is 1040 degrees Kelvin (769°C), assuming a stoichiometric mixture and complete combustion. Calculation of the flame temperature for n=6 is presented in Appendix A. Figure 1 demonstrates the temperature range available for generating steam as a function of the amount of water added. Note that temperatures on the order of 1000 to 2000 degrees Kelvin are generated at pressures of the order of 5 to 10 megaPascals with modest additions of liquid water. These calculations were made for an ideal gas equation of state, with dissociation included. Several non-ideal calculations have shown these results to be reliable to one percent. Furthermore, dissociation is unimportant at temperatures below 2500 degrees Kelvin.

The design conditions are 10 moles/second of superheated steam at 10.45 Megapascal and 769°C. Therefore, the following proportions of hydrogen, oxygen and water must be combined.

$$2.5\ H_2 + 1.25\ O_2 + 7.5\ H_2O \rightarrow 10\ H_2O \qquad (3)$$

or in more meaningful units, 5 grams per second (gm/sec) of H_2 and 40 grams per second of O_2 must react, with injection of 135 grams per second of water to produce 180 grams per second (10 moles/sec) of superheated steam at 769°C. The actual steam temperature attained may be less than the ideal temperature of 769°C due to a number of factors including: non-stoichiometry, incomplete combustion and non-adiabatic conditions within the chamber. The stoichiometry of the mixture will depend upon the accuracy to which the H_2 and O_2 flow can be controlled. The completeness of combustion will depend upon the mixing and turbulence within the combustion chamber. However, hydrogen and oxygen are so highly reactive that complete combustion should result.

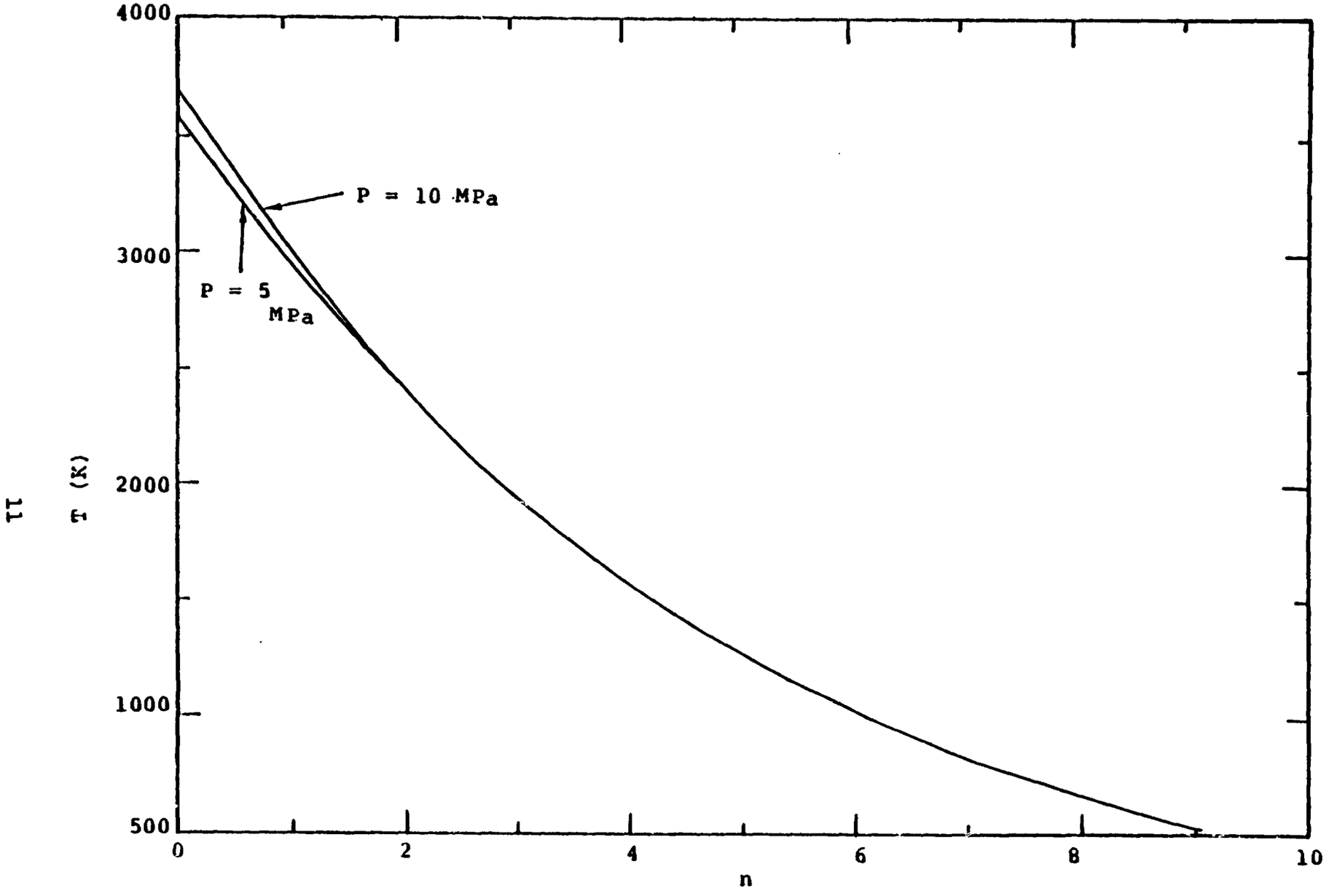

Figure 1. Adiabatic, constant pressure flame temperature ($\Delta H \equiv 0$) for $2H_2 + O_2 + nH_2O(\ell) \rightarrow (n+2)\ H_2O$ ideal gas equation of state assumed.

III. EQUIPMENT DESIGN

A mechanical flow diagram for the water-cooled hydrogen/oxygen steam generator is shown in Figure 2. This diagram schematically illustrates the pertinent equipment and instrumentation. A photograph of the overall test site is shown in Figure 3. The equipment design discussion is broken down into various subsystems. These systems include the pressure/combustion chamber, torch head, ignition system and water injection.

PRESSURE/COMBUSTION CHAMBER

The Pressure/Combustion chamber consists of a type 304 stainless steel cylinder with 10.2 centimeter thick heat treated carbon steel end plates. The chamber is made pressure tight by means of O-ring seals and proper torquing of the stud bolts which secure the end plates. A drawing of the pressure/combustion chamber is shown in Figure 4. The chamber is lined with a 5.1 centimeter thick layer of high temperature and moisture resistant thermal insulation to protect the pressure containing walls from the extreme heat and also to maintain adiabatic conditions within the chamber. The specifications for the insulation are tabulated in Appendix C. A 0.16 centimeter thick type 304 stainless steel liner is installed in the chamber to protect the thermal insulation from severe steam ablation and from becoming saturated with water which would cause it to lose its insulative properties. The liner also acts to help vaporize the water that impinges upon its hot surface. This liner is not pressure tight therefore the insulation is not subjected to a pressure gradient which would tend to crush it.

In addition, a J-type thermocouple is mounted on the outside wall of the chamber to monitor the surface temperature. This temperature is continuously indicated on a temperature readout instrument. Therefore, if the thermal insulation

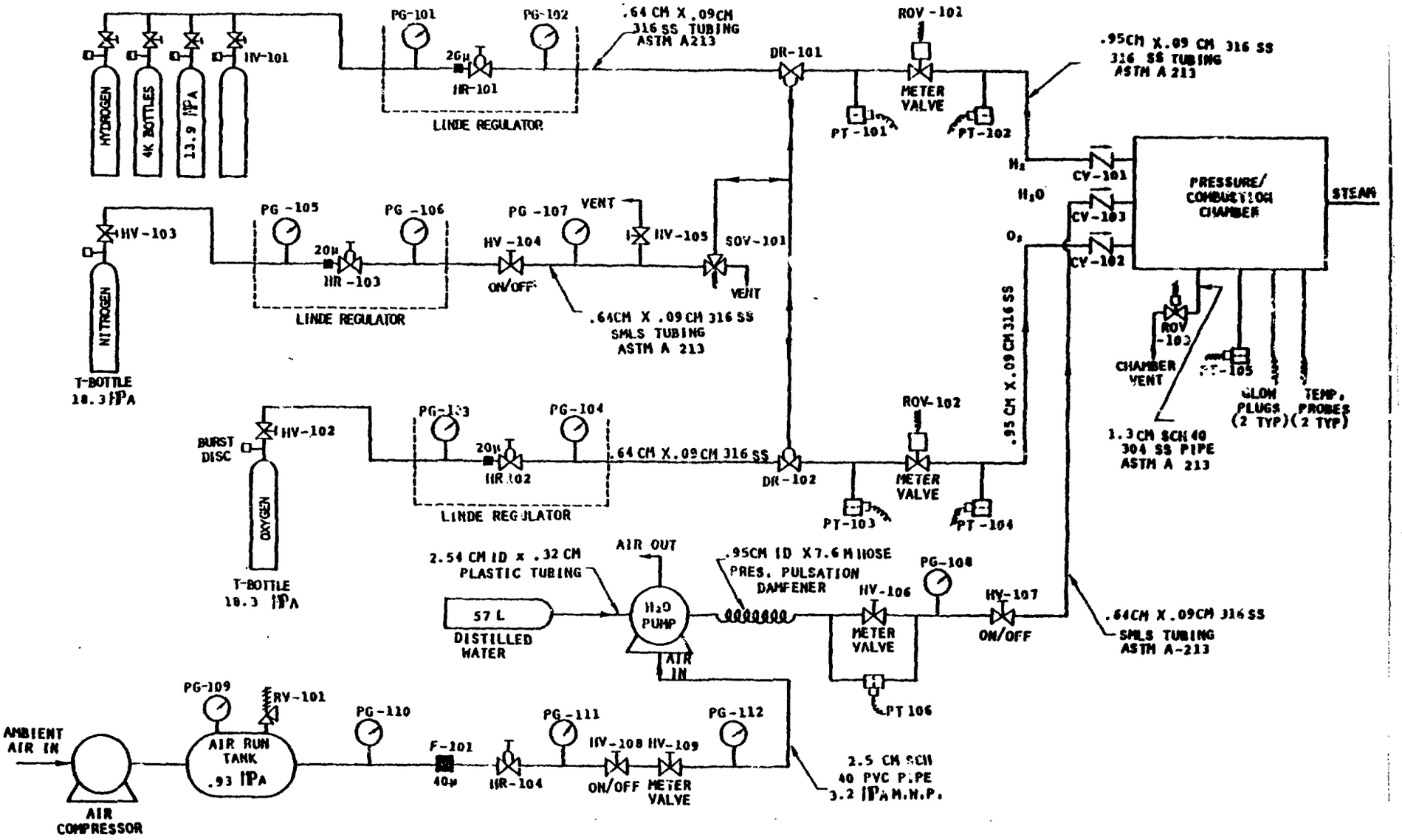

Figure 2. Flow Diagram for the H_2/O_2 Steam Generator.

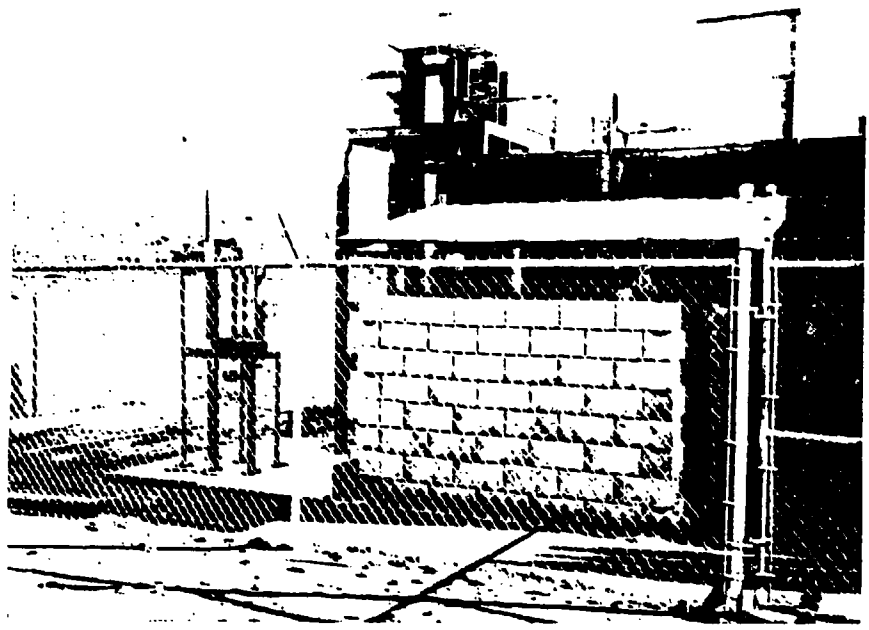

Figure 3. Overall view of the test site.

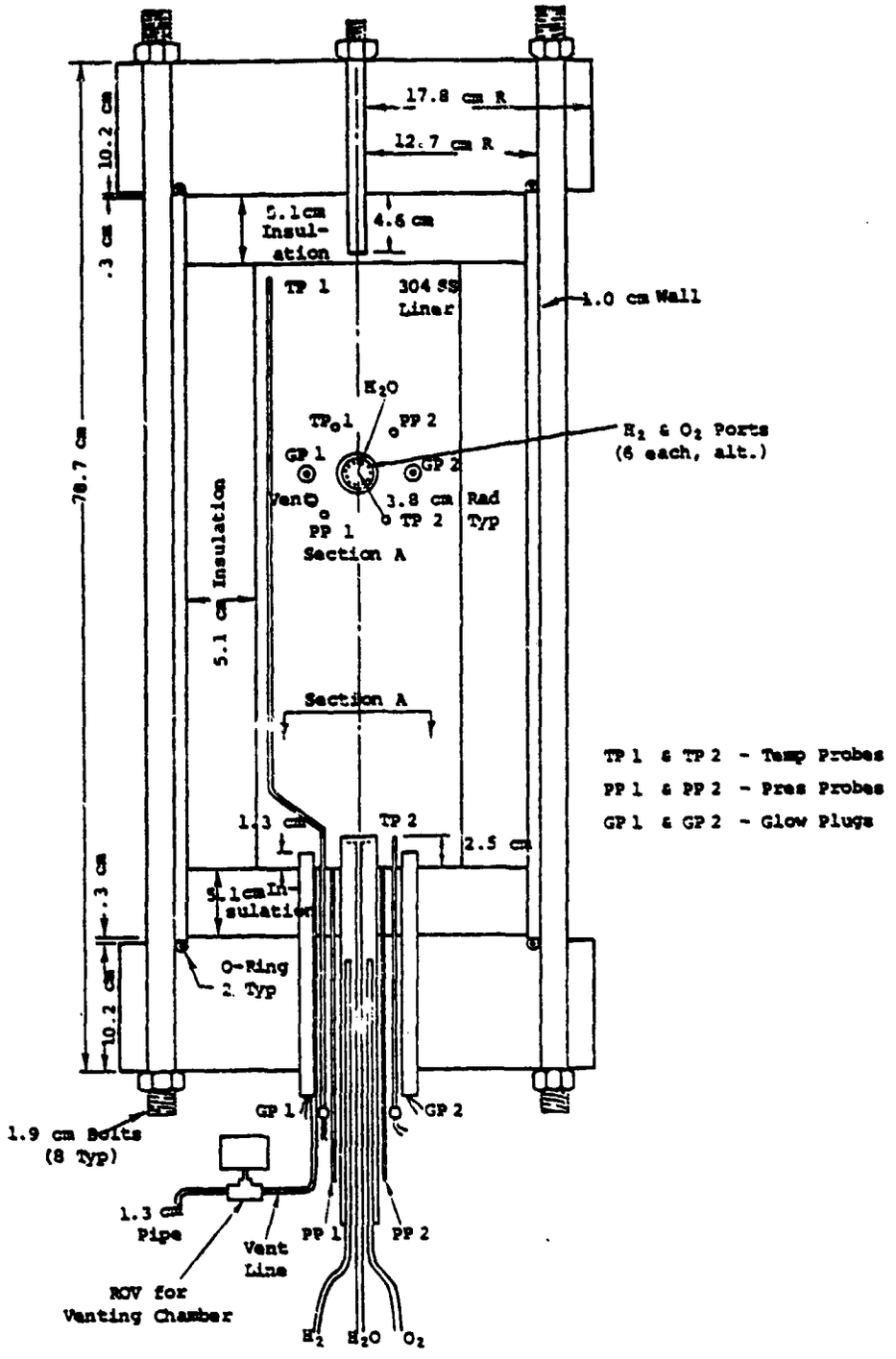

Figure 4. Steam generator chamber, 8803 cm^3 chamber volume.

should breakdown with subsequent over-heating of the chamber walls, the experiment can be aborted.

The chamber has a 1.3 cm stainless steel vent line with an electrically actuated valve (HOKE® two-way ball valve with a HOKE® electric motor driven actuator) for remote operation of the chamber vent mode from within the bunker.

The top end plate has a stainless steel post mounted in its center. This post has a small orifice (steam exit orifice) the size of which determines the steam pressure that can be attained. Sizing of this orifice is discussed in Section V.

Several photographs of the pressure/combustion chamber along with associated hardware are shown in Figures 5, 6, 7 and 8. Figure 5 shows an overall view of the chamber mounted on the test stand with a lifting hoist, which allows removal of the top end plate. Figure 6 is a photograph taken looking into the chamber. The thick annular band is the thermal insulation with the stainless steel protective liner. At the bottom of the chamber, notice the tip of the torch protruding through the center. Also note the glow plugs and the temperature and pressure probes. A photograph of the bottom of the chamber, showing the mounting of the torch with feed lines, vent line, thermocouples, pressure probe and glow plugs is shown in Figure 7. Figure 8 is a photograph of the thermal insulation and the stainless steel protective liner removed from the chamber.

TORCH HEAD

The torch head design is based on a commercially available, high-capacity scarfing and cutting torch (AIRCO 6200 series, style 822-6590 with a style 213, size 18 tip). This head was modified to include a water injection line ported through a central hole in the torch. The original purpose of the central hole was to allow flow of additional quantities of oxygen during the cutting process. A picture of this modified torch is shown in Figure 9.

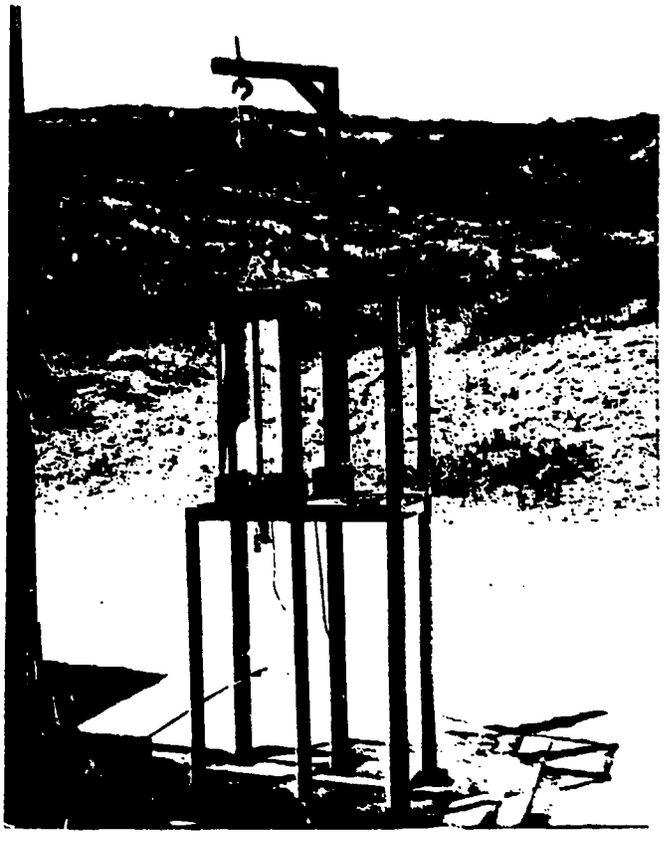

Figure 5. Overall view of chamber on test stand.

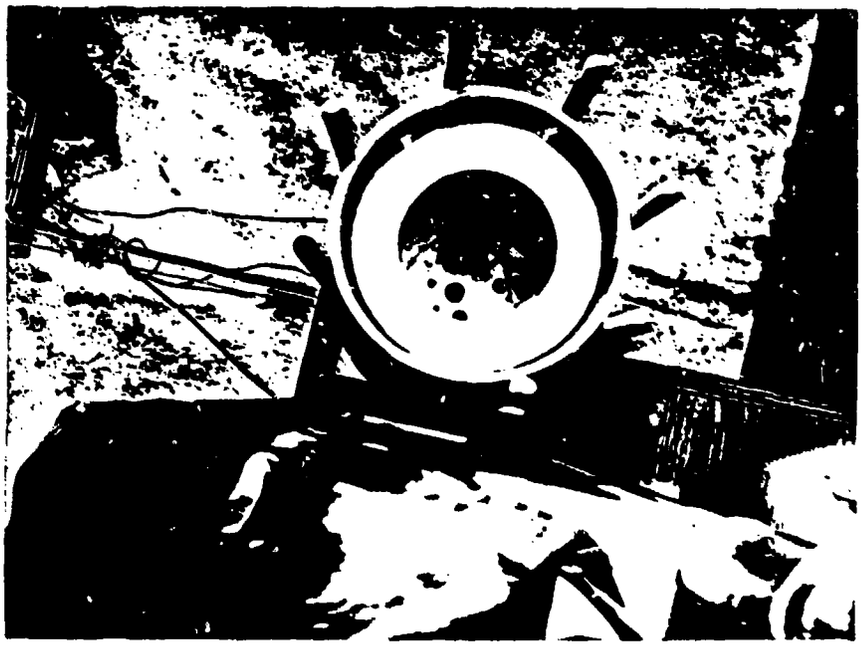

Figure 6. Test chamber (top view) showing ceramic insulation..

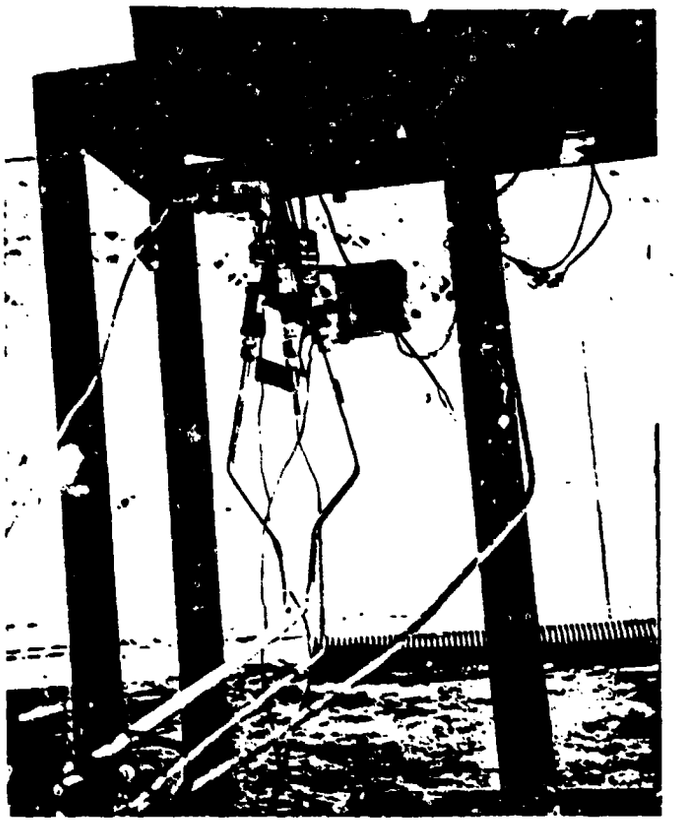

Figure 7. View of the bottom of the chamber.

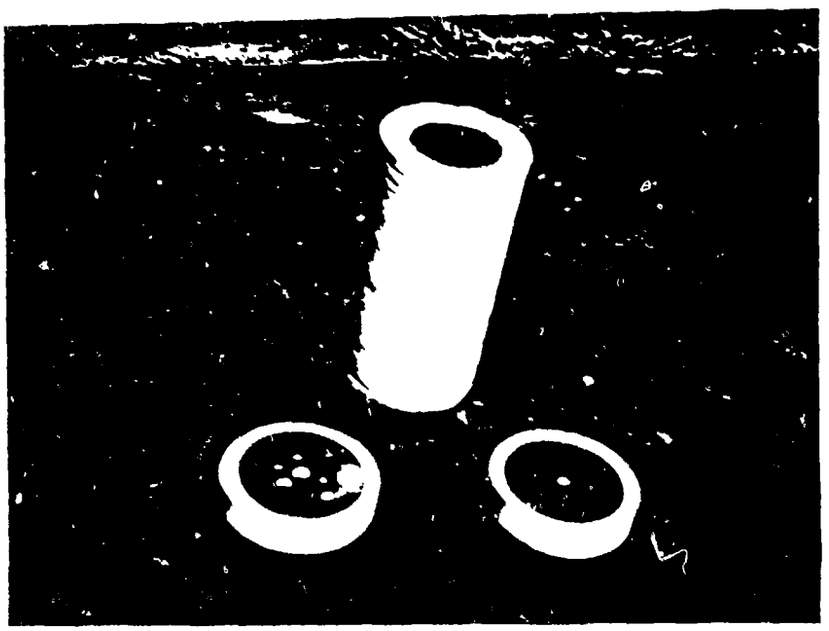

Figure 8. Thermal insulation and protective liner.

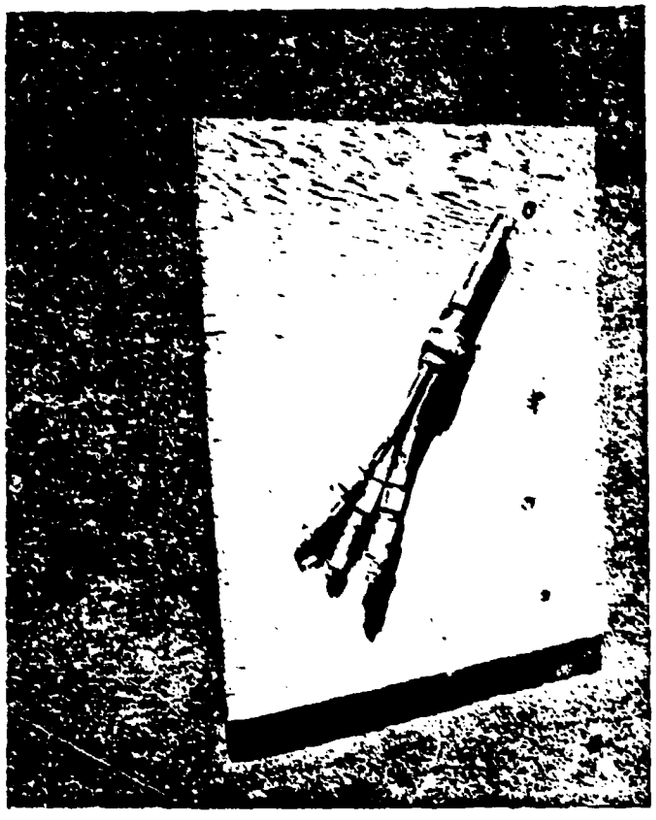

Figure 9. Torch head modified to accommodate water flow.

The tip for the torch was modified from a premixed (internally mixed) to an externally mixed type. In a premix or internal mix tip, the fuel and oxidizer mix and homogenize in the tip and exit as a combustible mixture. While in an external mix tip, the fuel and oxidizer exit as separate gases and mix outside the tip. In the premix configuration (used in work performed under Contract DNA001-77-C-0188), there were problems with flashback of the flame with subsequent catastrophic failure caused by melting of the copper tip. Flashback results when the back pressure in the chamber increases to such a value that the exit velocity of the mixture decreases to a value close to the flame velocity of the mixture. The flame velocity in a hydrogen-air mixture is about 300 cm/sec compared to about 40 cm/sec for methane and propane. The flame can thus flash back into the tip along the wall of the exit orifices where the gas velocity is a minimum. As the gas velocity decreases, the thickness of the boundary layer along the wall increases thus providing a wider path for flashback.

In an external mix type tip, there is very little chance of flashback. Since the fuel and oxidizer exit unmixed from independent orifices, there is not a combustible mixture within the tip to sustain a possible flashback flame. Even a mixture within the tip, resulting from possible diffusion of hydrogen back into an oxygen orifice, would be substantially below the lower flammability limit for hydrogen. A cross-sectional view of torch tip modified for external mixing is shown in Figure 10. This modification was accomplished by by silver soldering and/or peening closed alternate oxygen and hydrogen ports.

An external mix tip produces a diffusion type flame with no definite boundaries as opposed to a typical cone-shaped flame associated with a premix tip. Fortunately, hydrogen and oxygen are so highly reactive that essentially complete combustion is attained. Also the combustion chamber is relatively small, with intense turbulence and therefore provides thorough mixing.

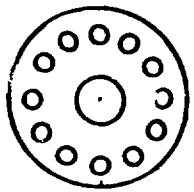

End
View

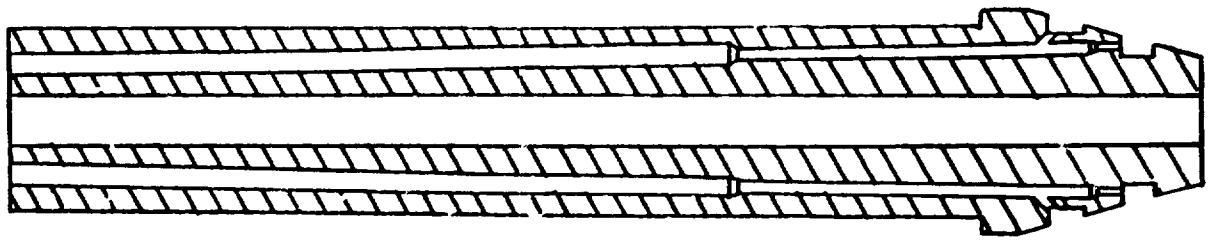

Cross-sectional View of Tip

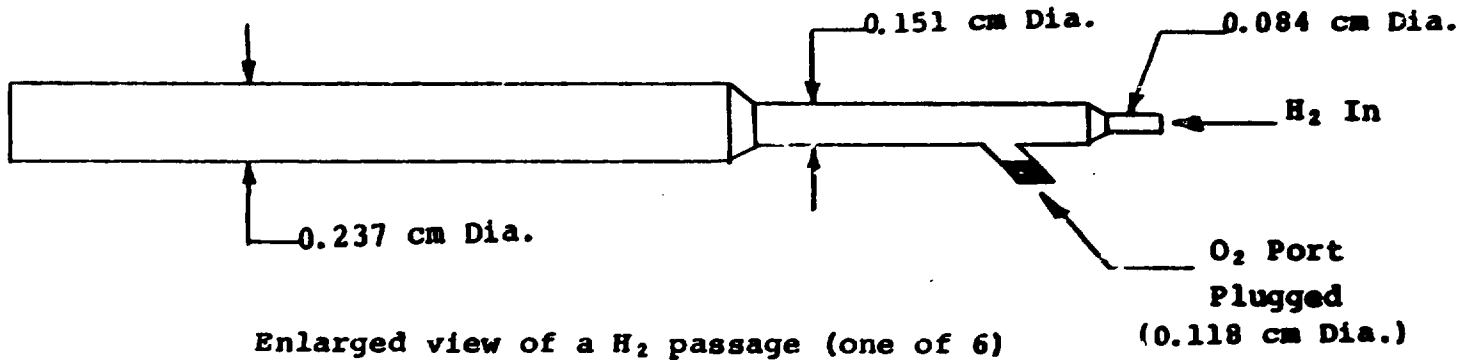

Enlarged view of a H_2 passage (one of 6)

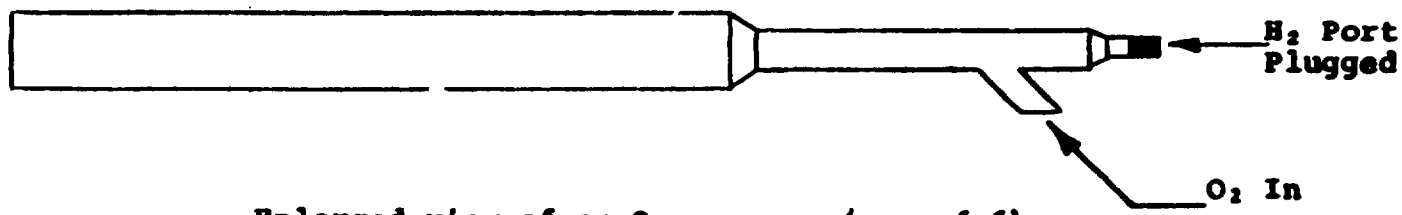

Enlarged view of an O_2 passage (one of 6)

Figure 10. Drawing of tip modified for external mixing.

Further modification of the tip included removing a factory provided circumferential skirt which acts as a flame holder. The flame holder tends to stabilize the flame by keeping it seated close to the tip preventing blow-off and possible quenching of the flame. In essence, a flame holder provides a large exit diameter and, therefore, a low exit velocity of the gas mixture. This new boundary layer, low gas velocity zone, acts as a pilot light to keep the main flame established as long as it is able to ignite the mixture flowing past. However, flame flashback results because of low exit velocity.

The torch assembly mounted in the combustion chamber is shown in Figure 7. The supply lines for hydrogen, oxygen and water, shown connected to the torch, are also shown in Figure 7. Notice that check valves are installed in all supply lines to prevent possible back-flow of water or gases into the supply lines.

IGNITION SYSTEM

The ignition source for enflaming the H_2/O_2 mixture is a redundant pair of model airplane glow plugs The glow plugs are small coiled platinum wires which incandesce (glow) when energized with a 6-volt dc source. They are mounted on aluminum posts with the electrical lead wires running through the center. The plugs are symmetrically disposed around the tip of the torch as shown in Figure 4. The ignition energy required to enflame an H_2/O_2 mixture, especially near stoichiometric, is very small (about 1/10th of that required for most hydrocarbon fuels) making the glow plugs very efficient igniters. A block diagram of the ignition system is shown in Figure 11.

WATER INJECTION

Water injection is maintain via a positive displacement, air-driven type pump (Haskel Model GSF-35 rated at 4.47 kilowatts). The water discharge rate is controlled by

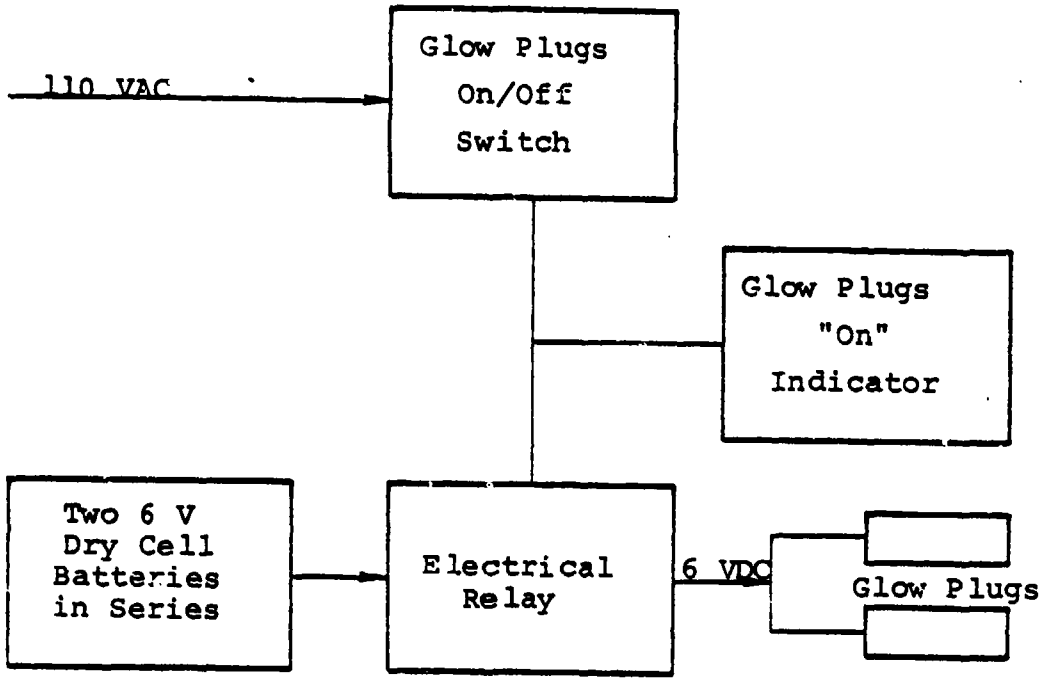

Figure 11. Block diagram of the ignition system.

regulating the air drive pressure and/or air flow rate to the pump. A precision metering valve (Whitey Model SS-6LRF4, 8 turn) is installed in the water line for further control of the water flow rate and discharge pressure. Distilled or de-ionized water is used to prevent possible hydrogen embrittlement of wetted metal surfaces in contact with hydrogen. Distilled water also minimizes corrosion and assures a clean system. A photograph of the control valves for the water flow is shown in Figure 12.

A pulsation dampener, consisting of a high pressure flexible hose 7.6 meters long and 0.95 centimeters in diameter formed into a coil, is installed at the pump discharge to dampen pressure spikes. This assures a more uniform water spray pattern in the combustion chamber and more accurate measurement of the water flowrate. The pulsation dampener also protects downstream plumbing from harmful pressure surges. A photograph of the water pump and pulsation dampener is shown in Figure 13.

Injection of the water into the combustion chamber requires that the water be broken up into very small droplets and distributed in a uniform pattern. As the droplet size decreases, the total surface area per unit volume for heat transfer increases, thus providing more rapid conversion to steam. The spray must be distributed uniformly into the flame so as to provide the greatest temperature gradient for heat transfer and also to assure of no localized hot spots. For a given flowrate, the droplet size varies directly with the orifice size and inversely with pressure.

After considerable experimentation with various spray nozzles, a combination of the proper orifice diameter and water pressure was obtained which provided a full cone spray pattern of small droplet size possessing the proper spray angle. This pattern engulfed the entire flame. For a given orifice size and pressure, the spray pattern and droplet size will vary somewhat

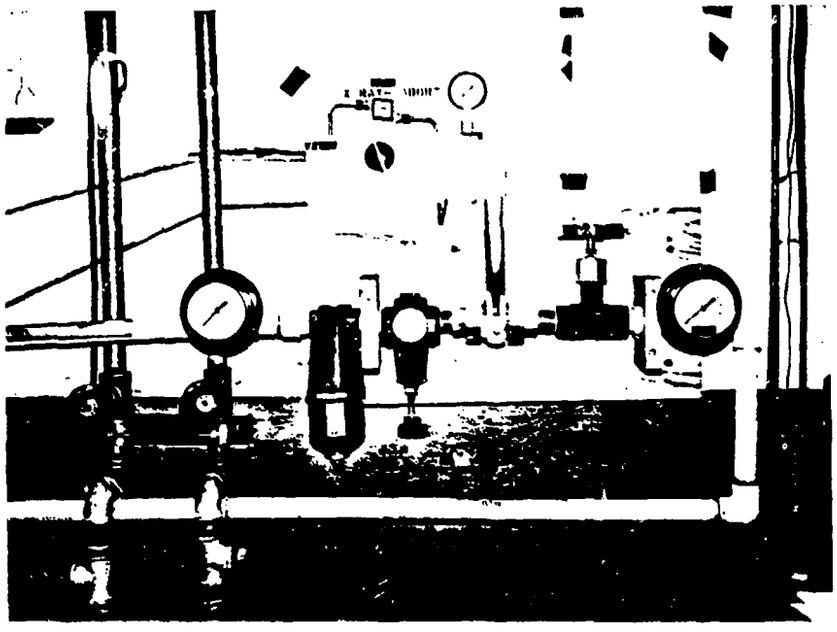

Figure 12. Controls for adjusting the water flow rate. (Notice the pressure regulator and flow control valve for controlling the air pressure and flowrate.)

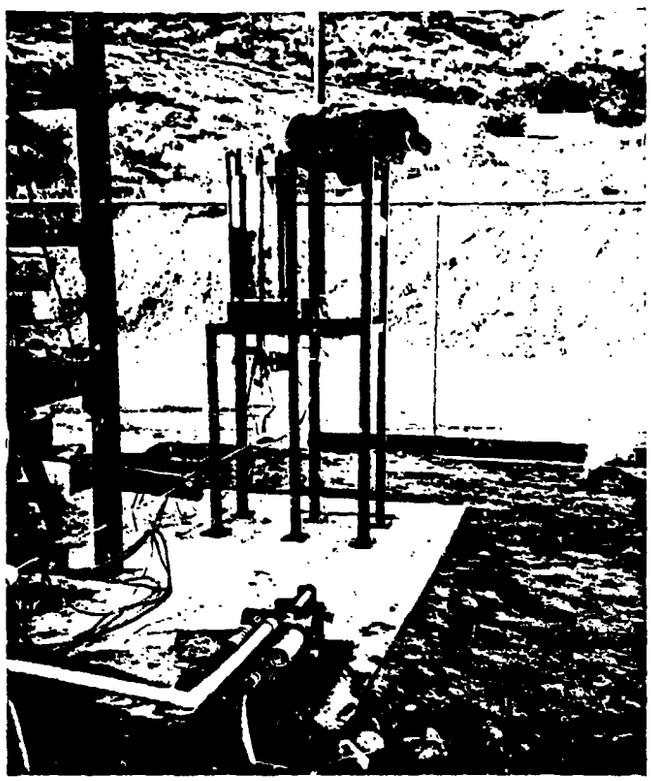

Figure 13. Water pump and pressure pulsation dampener.

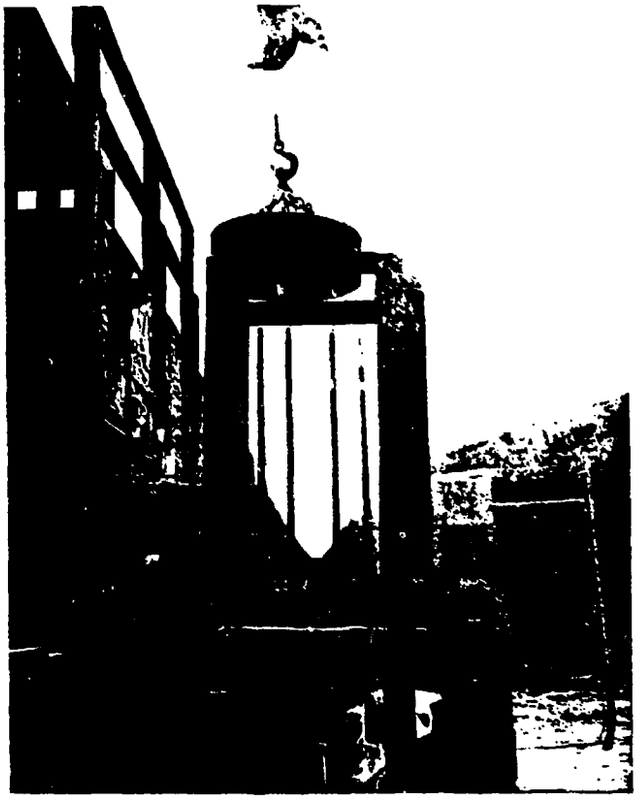

Figure 14. Water spray pattern.

with flowrate. For a flowrate of 8.14 l/min, atomization and a full cone spray pattern is obtained by maintaining a 6.9 MPa pressure drop across a 0.117 cm diameter orifice. A photograph of the resulting spray pattern is shown in Figure 14.

GAS SUPPLY

Four K-size bottles of hydrogen (5410 standard cubic liters at 13.9 MPa each) are manifolded together to provide a total run time of 1.4 minutes. One T-size bottle of oxygen (9345 standard cubic liters at 18.3 MPa) provides a run time of 1.9 minutes. These run times are based on flowrates 5 gm/sec and 40 gm/sec at 10.45 MPa, respectively, with final bottle decay pressure of 11.14 MPa. The location of the hydrogen and oxygen bottles is shown in Figure 3. They are outside any area which may be occupied by experimenters during an experiment. Only one person is permitted within the concrete block area when the gas bottles are connected and opened. The block area has a roof to shield the bottles from the sun. This sun shield assures a more constant temperature for the reactants and thus more accurate flow control.

ELECTRICAL EQUIPMENT DESIGN

Precautions were taken in selecting the electrical equipment that is exposed to a potential hydrogen enriched environment. The actuators for the hydrogen and oxygen flow control valves are housed in Nema type 7 enclosures and thus meet the National Electrical code requirements for a Class 1, Division II, Group D-type installation, hydrogen enriched environment. All other electrical valve actuators are intrinsically safe, inherently having no arc producing open contacts or switches, and thus also meet the NEC requirements. However, the entire steam generator assembly is located out-of-doors, thus, any free hydrogen from possible leaky connections, etc., diffuses away rapidly since there are no confining areas for hydrogen to concentrate.

IV. INSTRUMENTATION AND CONTROLS

Control of the entire experiment as well as monitoring of the thermodynamic conditions within the pressure/combustion chamber are effected from within the bunker. A photograph of the main control panel is shown in Figure 15.

PRESSURE REGULATION FOR H_2 AND O_2

The pressure of the hydrogen and oxygen is regulated in two stages for precise pressure control. The first stage regulation is by manually-set hand regulators (Linde Model SG3851, single stage). Second stage regulation is provided by dome regulators (Grove Mity-Mite Model 94) which are loaded remotely with nitrogen. The pressure to which the domes are loaded (pressurized) is directly related to the resulting delivery pressure for the hydrogen and oxygen. The dome regulators also act as remote shut-off valves. When the domes are not loaded, the dome regulators are "off," or in other words, there is no flow. The controls for the nitrogen are located inside the bunker, therefore, the experimenter has a positive means for remotely controlling the delivery pressure of hydrogen and oxygen from a safe area. The pressure control system for the hydrogen and oxygen is schematically illustrated in Figure 2. A photograph of the first and second stage pressure regulators is shown in Figure 16.

FLOWRATE CONTROL FOR H_2 AND O_2

The flowrates of the hydrogen and oxygen are controlled via digitally controlled metering valves. These digitally controlled valves consist of precision metering valves (Whitey Model SS-3NTRS4, 7 turn) with mounted stepping motors for remote actuation and valve positioning. The stepping motors convert electrical pulses into discrete mechanical rotational movements. For each pulse that is transmitted from a controller the shaft of the stepping motor rotates through one angular

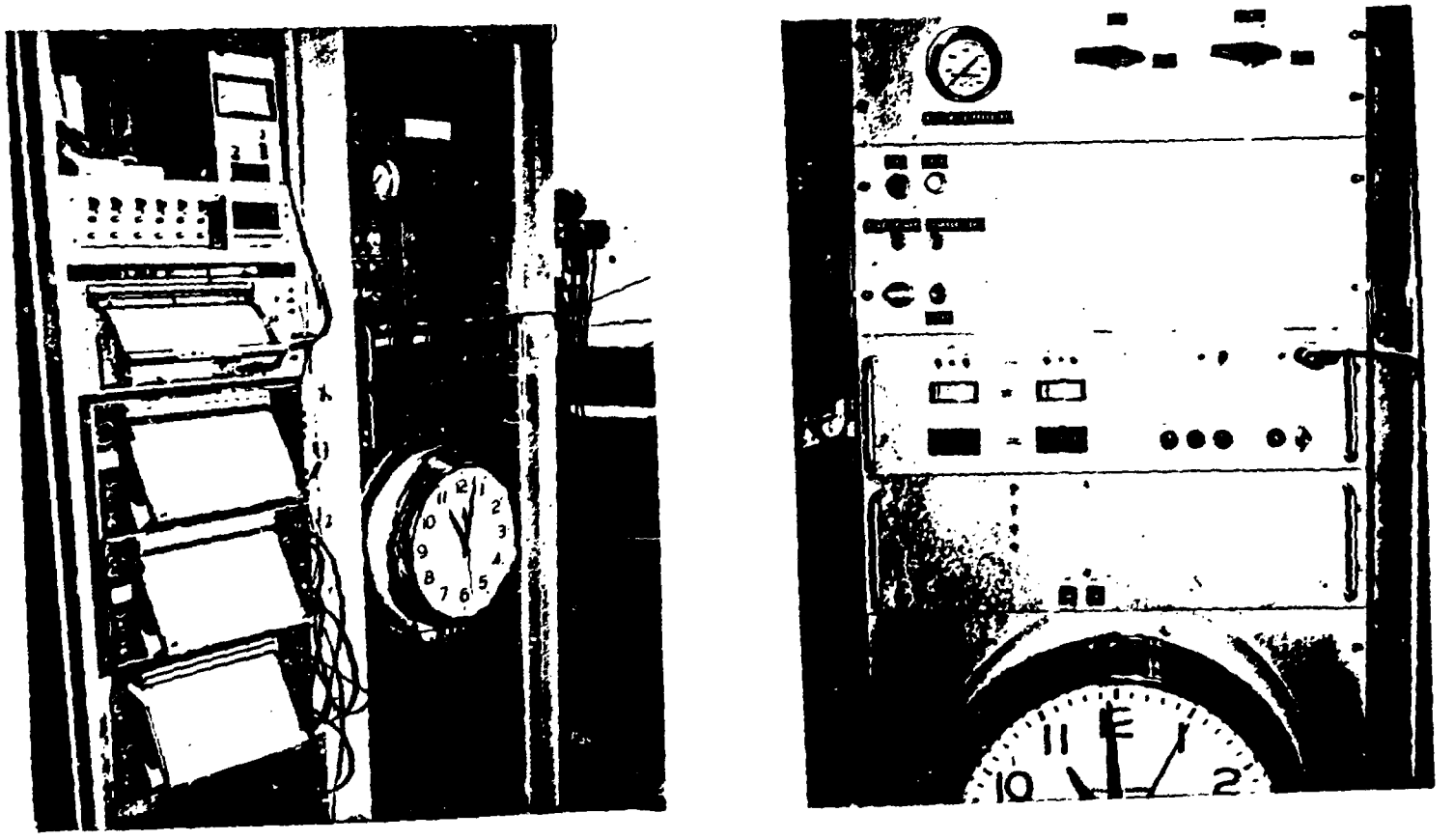

Figure 15. Control and recording module (close-up of controller).

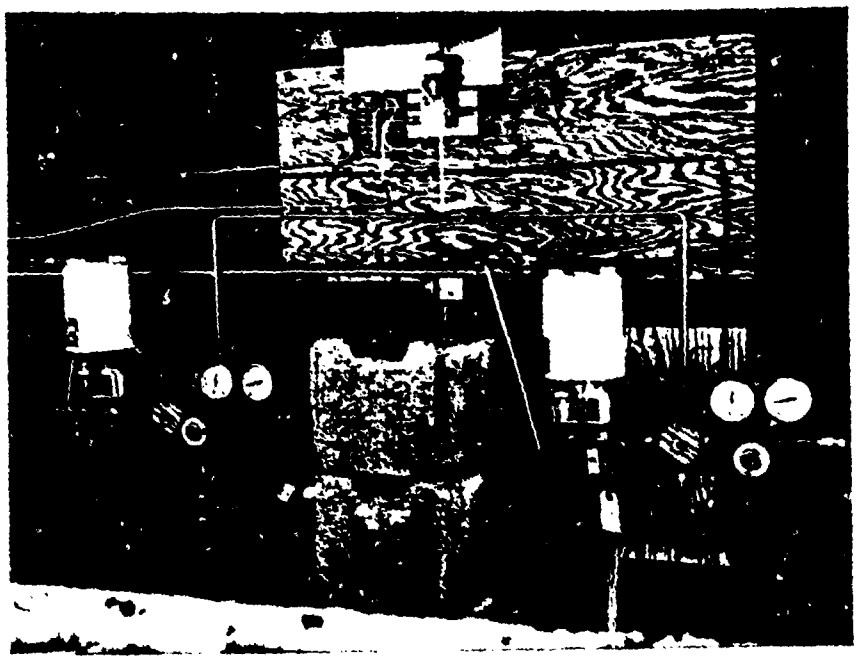

Figure 16. First and second stage regulators and digitally controlled metering valves mounted on-line (at the top of the picture, notice the solenoid valve for directing nitrogen to the dome regulators).

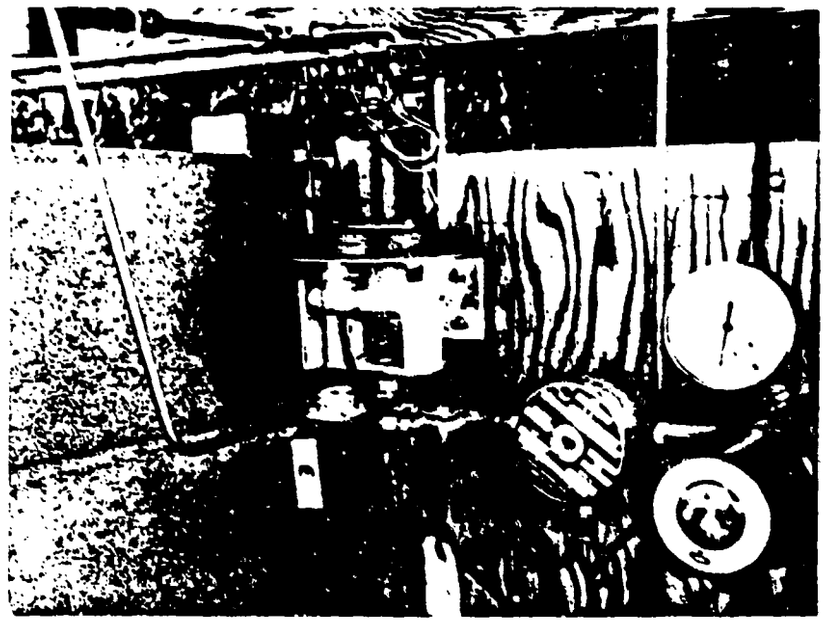

Figure 17. Close-up view of the stepping motor. (Notice the potentiometer geared directly to the shaft of the stepping motor in a 1:1 gear ratio.)

increment of motion, called the step angle. The step angle for these stepping motors is 0.9 degrees. There are 400 steps per revolution with a step accuracy of ± 3 percent, non-cumulative. This high resolution per revolution assures accurate positioning of the metering valves with excellent repeatability. The stepping rate can be as high as 1200 steps per second providing high speed positioning of the valves. The digitally controlled valves are shown in Figure 16. A photograph of a stepping motor with the explosion-proof housing removed is shown in Figure 17.

The valve controller has two identical channels, one each for the hydrogen and oxygen control valves. Each channel incorporates a digital clock to generate electrical pulses and an electronic counter to keep track of the number of pulses transmitted to the corresponding stepping motor. The number of steps of motion required (valve position) is programmed into the controller manually via three decades of thumbwheel switches. The sequencing and switching logic converts these programmed inputs into the proper signals and causes the stepping motor to step off the required motion. Each channel has a closed loop servo positioning circuit which compares the actual position with the command position and precisely moves the valve to the command position. This is accomplished via a potentiometer directly driven by the stepping motor. The voltage from the potentiometer is the analog equivalent of the stepping motor position while the input voltage is the analog equivalent of the digital input command set on the thumbwheel switches. If the voltage signal from the potentiometer does not coincide with the input voltage signal, the controller will drive the stepping motor until this error voltage (difference between input and potentiometer voltages) is zero. The valve is then in the position inputted by the thumbwheel switch. A meter is mounted on the front of the panel to indicate the valve position at any time. A drawing

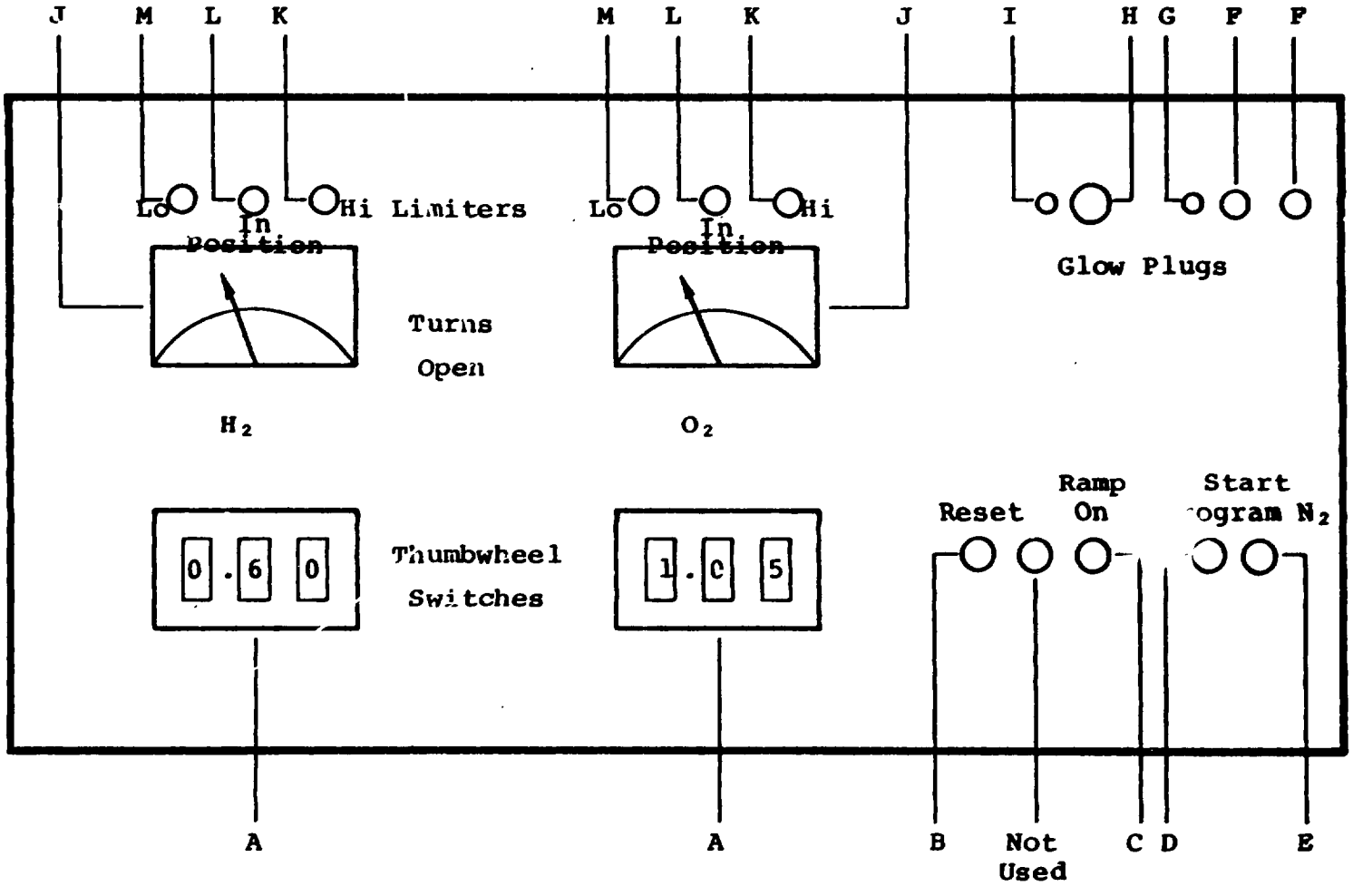

Figure 18. Drawing of the front panel of the controller.

of the controller panel with call out of all controls and indicators is shown in Figure 18. The function of the controls on the ont panel of the controller are described below.

A. Thumbwheel switches for entering the desired initial position for the hydrogen or oxygen metering valve to hundredths of one turn.

B. RESET - when the RESET button is pushed, the system will simultaneously return the hydrogen and oxygen valves to the position to which the thumbwheel switches are set.

C. RAMP ON - when the RAMP ON button is pushed, the system automatically and synchronously "ramps" the valves open further to positions dependent upon the preprogrammed ramps.

D. START PROGRAM - when the START PROGRAM button is pushed, the system simultaneously directs the digitally controlled valves to position to the number of turns open commanded by the thumbwheel settings.

E. SAFETY SWITCH, N_2. Toggle switch for activating the solenoid valve for loading and unloading the dome regulators.

F. OPERATOR'S SWITCH, N_2 (outlets for the operators switch). Abort type switch that must be continually held down to maintain the dome regulators loaded and thus flow of H_2 and O_2.

G. DOME REGULATORS LOADED INDICATOR lights up (red) when the domes are loaded.

H. GLOW PLUGS ON/OFF SWITCH. Turns the glow plugs on and off.

I. GLOW PLUG INDICATOR lights up (red) when the glow plugs are energized.

J. VALVE POSITION METER indicates the position of the valve in number of turns open.

K. HIGH LIMIT INDICATOR lights up (green) when the system tries without success to open the valve past a maximum number of turns as set on the thumbwheel switches. This is the maximum valve opening reference.

L. IN POSITION INDICATOR. When the system has achieved the command position as entered on the thumbwheel switches, the IN POSITION INDICATOR will light up (red).

M. LOW LIMIT INDICATOR lights up (green) when the system tries without success to close the valve past a minimum number of turns open as set on the thumbwheel switches. This is the zero reference point.

In addition, each channel includes a ramp circuit for opening the valves to a preprogrammed position. To maintain combustion stoichiometry the flowrates of hydrogen and oxygen are in a ratio of 2:1 on a molar basis, therefore the valve settings must be such to maintain this ratio. Consequently the ramps as well as the initial valve setting (thumbwheel switch setting) for the hydrogen and oxygen are different to maintain stoichiometry throughout the transition from critical flow to subcritical flow. The flow analysis through the valves will be explained further in Section V.

The ramps for both the hydrogen and oxygen control channels are run synchronously by the same electronic clock. Therefore, both valves reach the final valve settings simultaneously, thus maintaining stoichiometry. The ramp can be reprogrammed via minor circuit adjustments, providing a broader range of process flow conditions. A block diagram of the controller is shown in Figure 19.

PRESSURE AND TEMPERATURE MONITORING

Pressures are monitored using Validyne pressure transducers (Model DP-15, variable reluctance type) of the

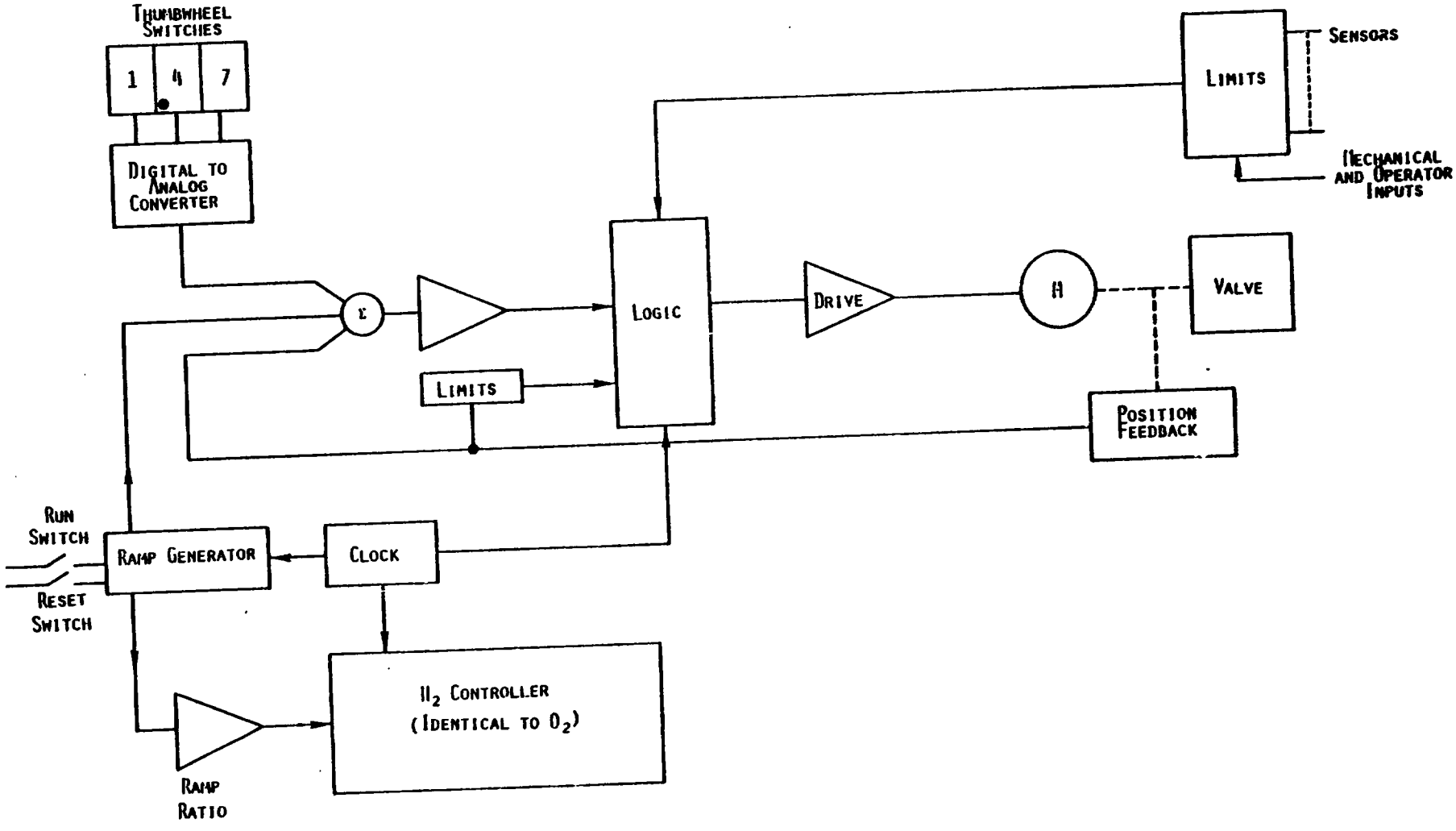

Figure 19. Functional block diagram of the controller for digitally controlled valves.

1. Pressure Monitoring (6 Channels)

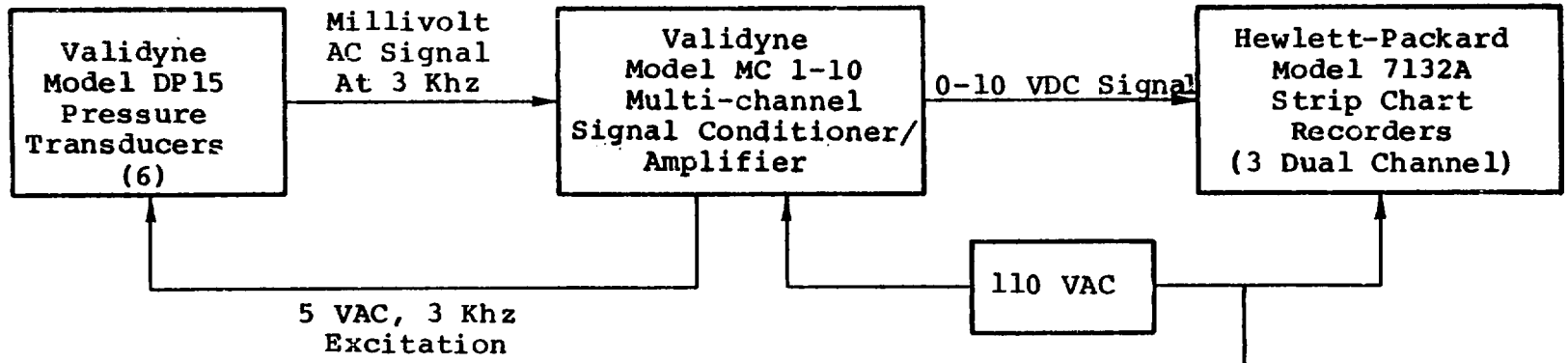

2. Temperature Monitoring (2 Channels)

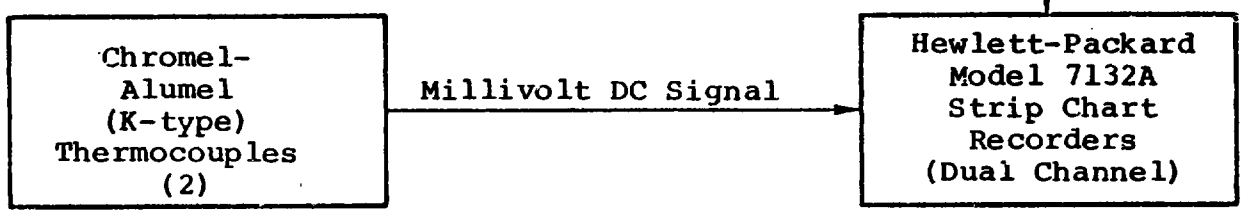

Figure 20. Block diagram of the pressure and temperature monitoring and recording systems.

appropriate range. The pressure upstream and downstream of the hydrogen and oxygen flow control valves as well as the differential pressure across the water flow control valve are monitored and recorded. In addition, the pressure within the chamber is continually monitored. Pressure communication to the chamber is effected by means of a stainless steel probe which extends through the bottom end plate and on into the chamber. A block diagram depicting the pressure monitoring and recording system is shown in Figure 20.

Two K-type thermocouples (Chromel-Alumel) with Type 316 stainless steel protective sheaths were used to monitor the temperature within the combustion chamber. The thermocouples extend through the bottom end plate into the chamber, one extending to a height equal to that of the torch tip and the other extending to the top of the chamber. Thus, the temperature at the two ends of the chamber is continually monitored and recorded. The temperature gradient as indicated by the two thermocouples indicates the effectiveness of the injected water in controlling the flame temperature. A block diagram or the temperature monitoring and recording system is shown in Figure 20. An ice reference junction was not used since the absolute error for measurements in the range of 800° - 1100° K is small (approximately 21° K).

The flow of nitrogen to the dome regulators is controlled via a solenoid valve. When energized, it directs flow of nitrogen to the dome regulators, which in turn, allow flow of H_2 and O_2. When de-energized, it unloads the domes by diverting the nitrogen from the domes through a vent. In the event of a power failure during the course of the experiment, the solenoid valve would stop the flow of hydrogen and oxygen to the torch. A block diagram of the control system for loading and unloading the dome regulators is shown in Figure 21.

In addition, an intercom system is located near the torch head to monitor noises from the chamber or surrounding

area. The flow of gas, ignition, as well as problem noises can be heard from within the bunker. This intercom proved to be worthwhile on several occasions, by preventing a possible meltdown.

One experiment was aborted after 20 seconds into the run because of abnormal combustion noises. A slight anomalous drop in the chamber pressure and temperature corresponded with these abnormal noises. Upon examination of the interior of the test chamber, the copper torch tip was completely melted and and had pieces of copper imbedded in the walls of the thermal insulation. This catastrophic failure of the torch tip was a result of flame flashback into the tip. Subsequently, the tip was redesigned to an external mix type to circumvent flame flashback problems.

Another experiment was aborted after 45 seconds because of abnormal noises from the chamber which corresponded with pressure and temperature spikes. The steam exit orifice was found to be plugged with chips of ceramic insulation. Subsequently, a type 304 stainless steel liner was installed to prevent ablation of the thermal insulation.

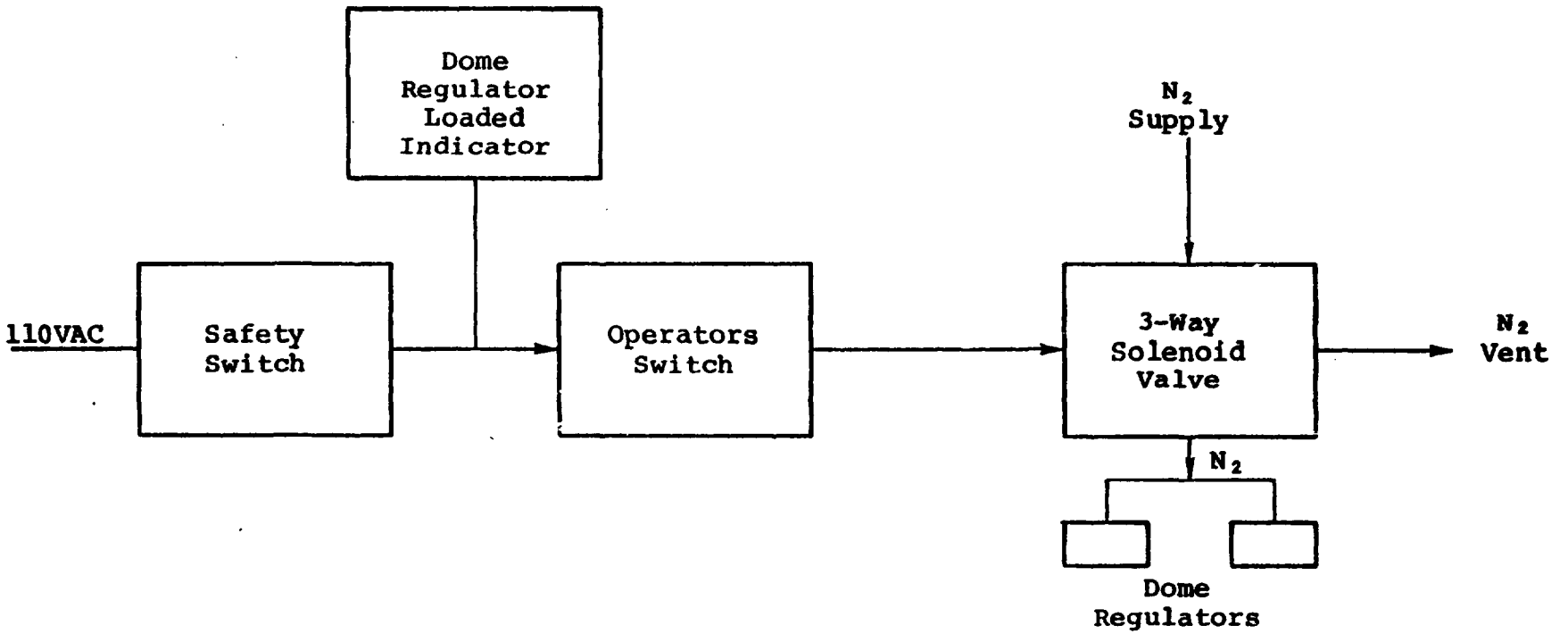

Figure 21. Block diagram of the dome regulators control system.

V. PROCESS CONTROL

The design process conditions are to produce 10 moles/sec of superheated steam at 769°C and 10.45 MPa. As stated previously, the flowrates of the reactants to produce 10 moles/sec of steam at 769°C are as follows: H_2 - 5 gm/sec, O_2 - 40 gm/sec, and H_2O - 135 gm/sec. The desired pressure of 10.45 MPa can be attained by proper sizing of the steam exit orifice in the pressure/combustion chamber. Figure 22 below illustrates the flow process.

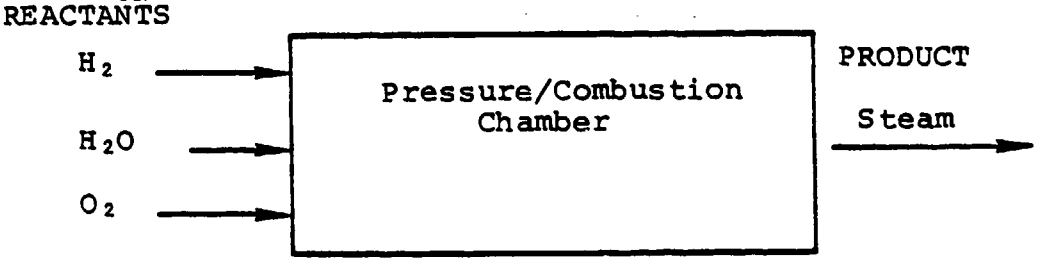

Figure 22. Process flow diagram.

Initially the pressure within the chamber will be at atmospheric pressure with the flowrate of steam being zero. As flow of the reactants initiates with subsequent combustion, the pressure in the chamber will increase. The flowrate of the steam will also increase since the density is increasing accordingly. As the chamber pressure approaches 10.45 MPa, the steam mass flowrate will be such that it is equal to the combined mass flowrates of all the reactants. This is assuming 100% quality steam. The pressure and flowrate of the steam as a function of time are shown in Figures 23 and 24 respectively.

SIZING OF THE STEAM EXIT ORIFICE

Calculation of the steam exit orifice in the test chamber required to attain 10.45 MPa steam at a flowrate of 10 moles/sec and at 769°C is as follows. The flow of the steam through the exit is initially subcritical but as the chamber pressure, P_c, increases to a value greater than 1.89 times the back pressure, ($P_b/P_c < 0.528$), the flow transits

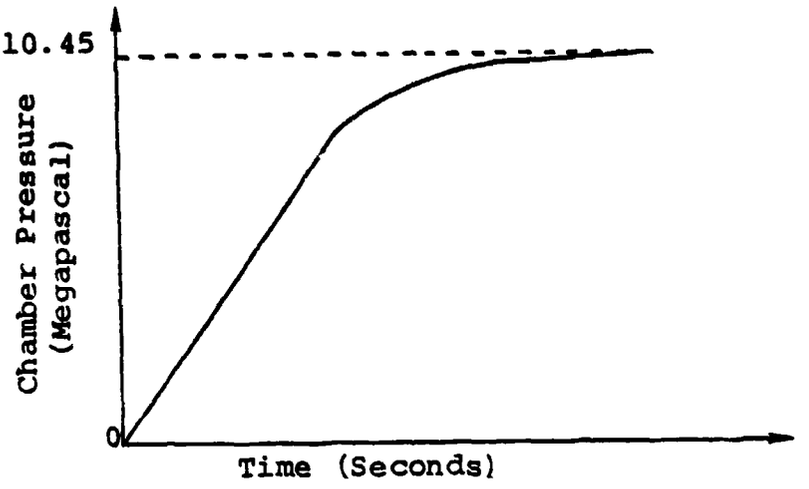

Figure 23. Chamber pressure versus time.

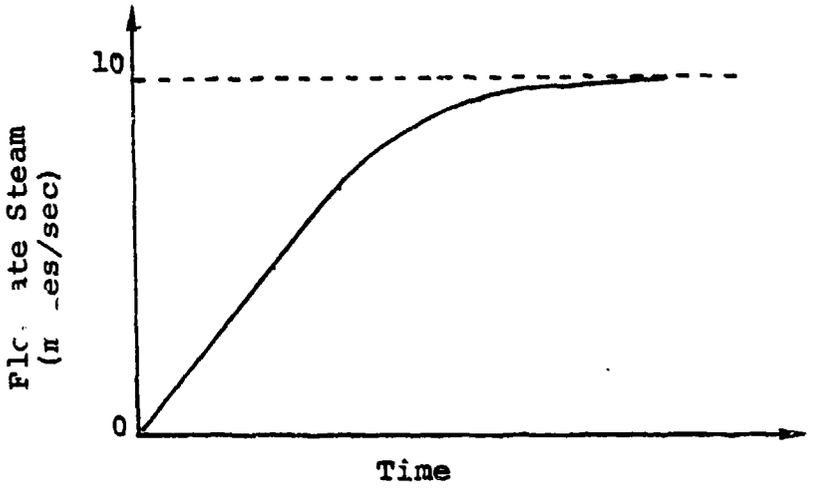

Figure 24. Flowrate of steam versus time.

to critical flow. The back pressure being atmospheric and therefore constant. Critical flow of a compressible gas is defined as flow that results when the ratio of the back pressure to the chamber pressure is less than the critical pressure ratio, which is 0.528 for an ideal gas. This also implies that the flow velocity at the exit of the orifice is Mach 1 or sonic. In other words, the flow velocity is equal to the velocity of sound through the particular gas.

Therefore, the flow of steam is choked at all times, except during the initial period of time in which the flow is subcritical; that is, until the chamber pressure reaches 0.192 MPa.

The mass flowrate of a gas can be expressed by the continuity equation

$$\dot{m} = \rho VA \qquad (4)$$

where:

$\dot{m}$ = mass flowrate (gm/sec)

ρ = mass density (gm/cm^3)

V = velocity of flow (cm/sec)

A = cross-sectional area of orifice (cm^2)

The density can be derived from the equation of state for an ideal gas

$$\rho = P/RT \qquad (5)$$

where:

P = absolute pressure (MPa)

R = gas constant (.1103 gm-cal/gm-°K for steam)

T = absolute temperature (°K).

As was stated previously, for critical flow the flow velocity is sonic since the Mach number is equal to one at the orifice. Mach number being expressed as:

$$M = V/C \qquad (5)$$

where:

M = Mach number, dimensionless

V = flow velocity

C = speed of sound through the gas.

The speed of sound through a gas being defined by

$$C = \sqrt{\gamma g_c RT} \tag{7}$$

where:

γ = ratio of the constant pressure and constant volume specific heats, C_p/C_v, 1.4 for steam

g_c = gravitational constant, 1 gm-cm/dyne-sec^2.

Equations 5 and 7 are substituted into Equation 4 to give the relation

$$\dot{m} = \frac{p}{RT} \sqrt{\gamma g_c RT}\ A \tag{8}$$

The velocity term in this expression (Equation 8) represents the velocity through the orifice. The temperature and pressure at the orifice must be used to determine the mass flowrate.

For the flow of a compressible gas through an orifice, isentropic flow can be assumed. Isentropic flow being defined as adiabatic and reversible, frictionless. Also in an isentropic process, the stagnation pressure and temperature are constant. The stagnation pressure and temperature are expressed by Equations 9 and 10, respectively.

$$P_t = P\left(1 + \frac{\gamma-1}{2} M^2\right)^{\frac{\gamma}{\gamma-1}} \tag{9}$$

$$T_t = T\left(1 + \frac{\gamma-1}{2} M^2\right) \tag{10}$$

where:

P_t = stagnation pressure

P = static pressure

T_t = stagnation temperature

T = static temperature

γ = ratio of specific heats, 1.4 for an ideal gas

M = mach number

For an ideal gas flowing at Mach 1, these reduce to

$$P = 0.528P_t \tag{11}$$

$$T = 0.833T_t \tag{12}$$

The flow velocity within the chamber can be assumed to be essentially zero. Therefore, the stagnation pressure and temperature are equal to the static pressure and temperature inside the chamber, respectively. Consequently, since the pressure and temperature inside the chamber are measured and thus of known values, the static pressure and temperature at the orifice can be determined from Equations 11 and 12.

Substituting Equations 11 and 12 in Equation 8 gives the expression:

$$\dot{m} = \frac{0.528P_t}{R \times 0.833T_t}\sqrt{\gamma g_c R \times 0.833T_t}\quad A \tag{13}$$

From this expression the required orifice size for any combination of steam flowrates, temperatures and pressures can be derived, provided the flow is sonic at the exit orifice. The orifice size for generating 10 moles/sec (180 gm/sec) at 700°C at 10.45 MPa, after substituting the proper values in Equation 13 and in the proper units, is 0.46 cm in diameter. The orifice size is a fixed parameter which can not be changed during the course of an experiment; therefore, if the flowrates of the reactants and/or the steam temperature are too low, the chamber will not reach the desired pressure. Of course, if the quality of the steam is not 100%, neither the steam flowrate or pressure will be as high as expected. However, should the steam temperature and/or the flowrates of the reactants be too high, all other variables remaining constant, the chamber pressure will increase to reflect these increases.

FLOW ANALYSIS OF H_2 AND O_2

The flowrates of the hydrogen and oxygen are controlled via servo-controlled metering valves. The inlet pressure to the metering valves is maintained constant via the dome pressure regulators. This pressure, P_1, being maintained at 11.14 MPa for generating 10.45 MPa steam. A flow diagram for this process is shown in Figure 25.

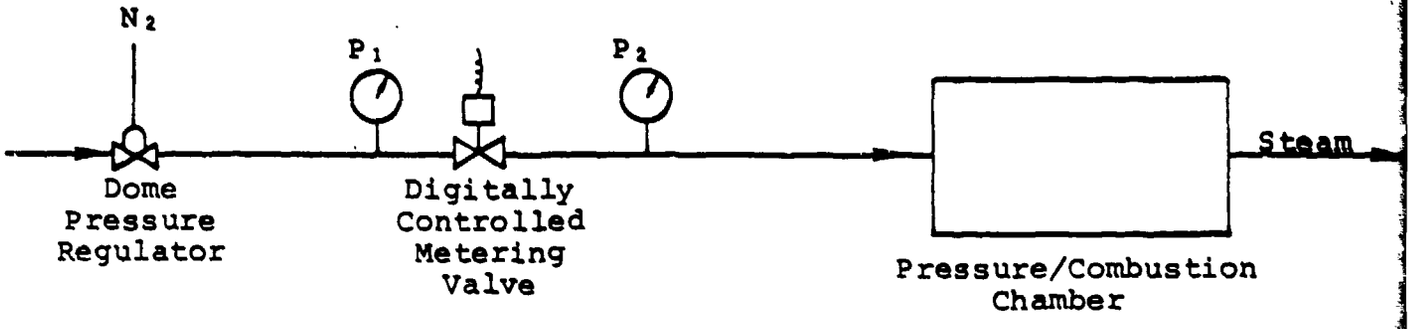

Figure 25. Typical flow diagram for hydrogen and oxygen.

Initially the flow through the metering valves will be critical and will remain choked until the back pressure or chamber pressure increases to 5.88 MPa, that is, until the critical pressure ratio P_2/P_1 exceeds 0.528. During this period of time in which the flow is critical, the flowrates of the hydrogen and oxygen remain constant at 5 gm/sec and 40 gm/sec respectively since the supply pressure is maintained constant at 11.14 MPa. The changing, increasing, back pressure has no influence upon the flowrates as long as the flow is critical. This can be explained from the continuity equation, $m = \rho VA$. The density is constant since the pressure is fixed at 11.14 MPa, also the velocity is constant at the sonic velocity and the area is fixed since the metering valve setting is preset by the thumbwheel switches.

As the chamber pressure increases to a value greater than 5.88 MPa, the flow goes subcritical since the critical pressure ratio is exceeded, that is, $P_2/P_1 > 0.528$. Therefore, the flow velocity decreases, becoming subsonic with an ultimate decrease in the flowrates. The flowrates of the hydrogen and

oxygen will decrease until the flow of the steam reaches steady-state, steady flow conditions, which is dependent upon the final chamber pressure and temperature as well as the steam exit orifice size. The flow analysis through the metering valves is depicted graphically in Figures 26 and 27.

To maintain the flowrates of the hydrogen and oxygen constant at 5 gm/sec and 40 gm/sec respectively, the metering valves must be opened further as soon as the flow goes sub-critical. Opening of the valves must continue until steady-state, steady flow conditions of 10 moles/sec of superheated steam at 769°C and 10.45 MPa is attained. Calculation of the initial and final settings for the hydrogen and oxygen valve are shown below.

The universal yardstick for the flow capacity of a valve is the flow coefficient, C_V. The flow coefficient is defined as the flow which will pass through a given flow restriction for a given pressure drop.

The flow coefficient, C_V, for critical flow through a valve is expressed by

$$C_V = \frac{Q\sqrt{SG \times T}}{694\ P_1} \qquad (14)$$

where:

C_V = flow coefficient, dimensionless
Q = flowrate, l/sec @ STP
SG = specific gravity, dimensionless
T = absolute temperature, °K
P_1 = inlet or supply pressure, absolute (MPa)

For flowrates of 5 gm/sec of hydrogen and 40 gm/sec of oxygen at 11.14 MPa and 21°C, the required flow coefficients are 0.033 and 0.066 respectively. These flow coefficients correspond to valve settings of 0.6 turns open for the hydrogen valve and 1.05 turns open for the oxygen valve. These valve settings are determined from the calibration curves of the valves shown in Figures B-1 and B-2 of Appendix B.

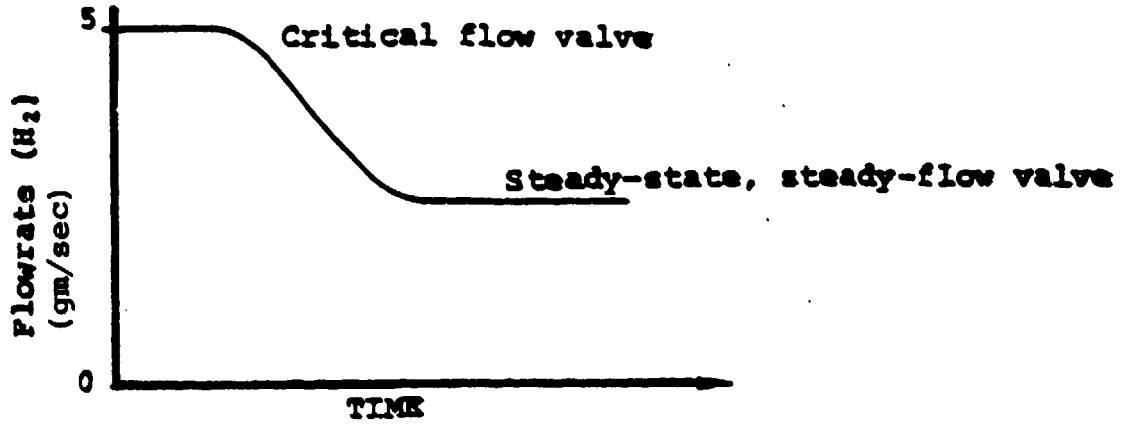

Figure 26. Flowrate of H_2 versus time with P_1 at 11.14 MPa and a fixed valve setting.

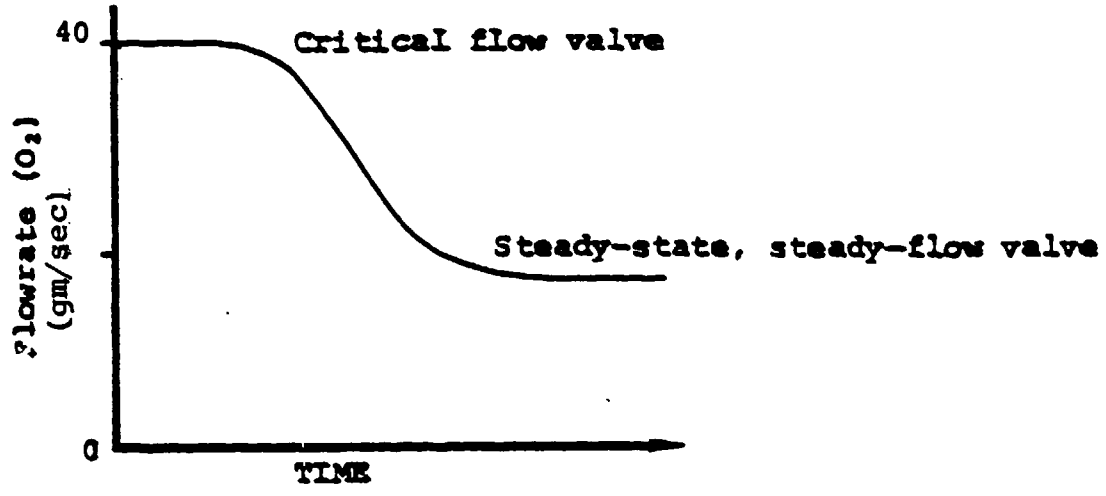

Figure 27. Flowrate of O_2 versus time with P_1 at 11.14 MPa and a fixed valve setting.

The flow coefficient for subcritical flow through a valve is expressed by

$$C_V = \frac{Q}{819}\sqrt{\frac{SG \times T}{P_1^2 - P_2^2}} \qquad (15)$$

where:

P_1 = inlet or supply pressure to valve, absolute (MPa)

P_2 = outlet pressure of valve, absolute (MPa)

For flowrates of 5 gm/sec of hydrogen and 40 gm/sec of oxygen at 11.14 MPa and 21°C and allowing a 0.34 MPa pressure drop across each valve, that is, P_2 equals 10.8 MPa, the required flow coefficients are 0.114 and 0.228 respectively. These flow coefficients correspond to valve settings of 2.4 turns open for the hydrogen valve and 5.5 turns open for the oxygen valve (as determined from the calibration curves). These are the ultimate valve settings that must be achieved to attain the steady-state, steady flow conditions of 10 moles/sec of steam at 10.45 MPa and 769°C.

The steady-state, steady flow conditions are attained via automatic ramp circuits which are a built-in feature of the controller for the digitally controlled metering valves. The ramp circuits synchronously ramp the metering valves open to the final settings in 30 seconds. The ramps for the hydrogen and oxygen valves are shown in Figure 28.

The ramps will not track the flowrates perfectly. The actual hydrogen and oxygen flowrates will overshoot and undershoot the desired flowrates of 5 gm/sec and 40 gm/sec, respectively. However, this overshooting and undershooting of the flowrates will not prevent achieving the desired steady-state, steady flow conditions for the steam. The flowrate of the water is maintained at the design flowrate of 135 gm/sec. This is the flowrate required to maintain the flame temperature at 769°C. Therefore, an overshoot in the flowrates would tend to cause the flame temperature to increase. However, the

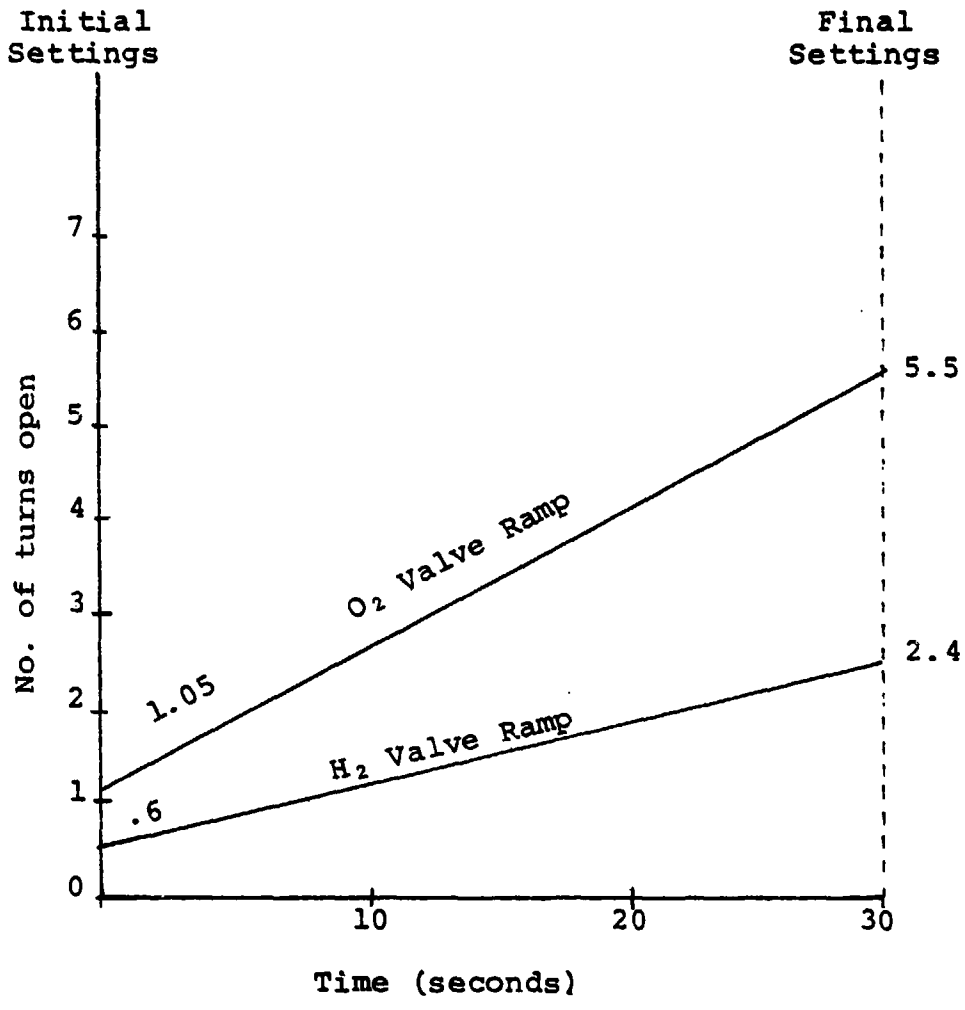

Figure 28. Ramps for increasing flow of hydrogen and oxygen as the chamber pressure increases.

effect of an overshoot upon the flame temperature is minor since the amplitude and duration of a given overshoot are small. Figure 29 conceptually illustrates this overshooting and undershooting of the flowrates.

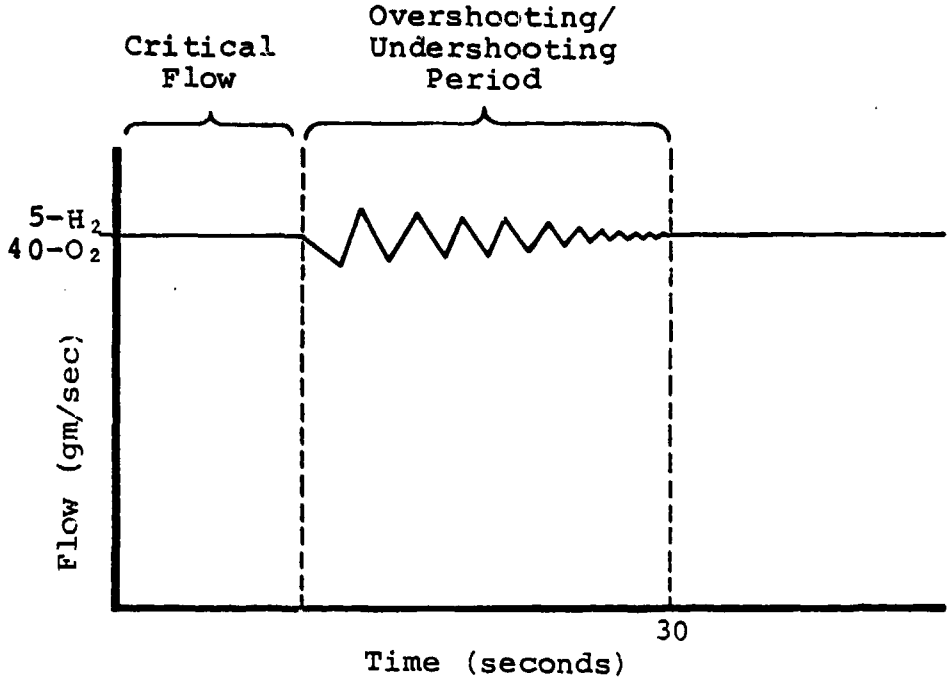

Figure 29. Conceptual illustration of the flowrates of H_2 and O_2 versus time.

The ramps must be initiated when the flow into the test chamber transits from critical to subcritical; that is, when the chamber pressure reaches 5.88 MPa. The time for the chamber pressure to reach 5.88 MPa can be calculated as shown below.

The conservation of mass states that the mass flowrates entering a control volume must be equal to the rate of change in the mass within the control volume plus the mass flowrate leaving the control volume. This relation can be expressed as:

$$\frac{dm_i}{dt} = \frac{dm_{CV}}{dt} + \frac{dm_e}{dt} \qquad (16)$$

where:

$\frac{dm_i}{dt}$ = mass flowrate into the control volume

$\frac{dm_{CV}}{dt}$ = rate of change of the mass within the control volume

$\frac{dm_e}{dt}$ = mass flowrate leaving the control volume

This relationship is illustrated pictorially in Figure 30.

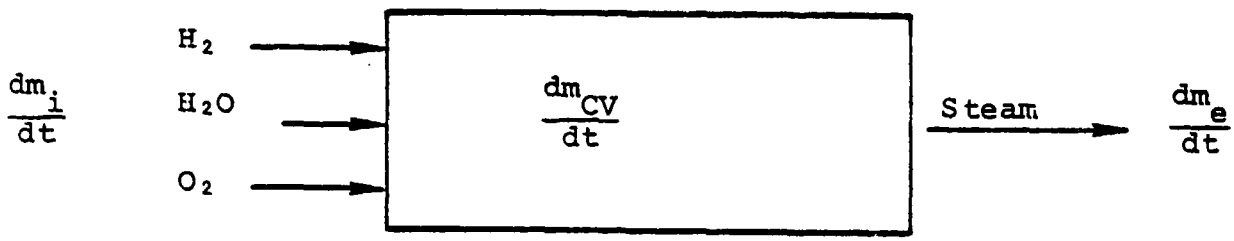

Figure 30. Illustration of the law of conservation of mass.

The total mass flowrate in can be expressed as:

$$\frac{dm_i}{dt} = \dot{\rho V})_{H_2} + \dot{\rho V})_{O_2} + \dot{\rho V})_{H_2O} \qquad (17)$$

Where:

ρ = mass density, gm/m^3

V = volumetric flowrate, l/sec

For flowrates of 5 gm/sec of H_2, 40 gm/sec of O_2 both at 11.14 MPa and 135 gm/sec of water

$$\frac{dm_i}{dt} = 180 \text{ gm/sec a constant} \qquad (18)$$

The mass flowrate of the steam leaving the chamber is a function of the chamber pressure assuming the temperature and the mass flowrate entering the chamber are constant. The

mass flowrate exiting the chamber is expressed by Equation 13, that is

$$\dot{m}_e = \frac{0.528P_t}{R \times 0.833T_t}\sqrt{\gamma g_c R \times 0.833T_t}\quad A \qquad (19)$$

Assuming a constant steam temperature of 769°C and a steam exit orifice of 0.46 cm, mass flowrate leaving can be expressed as a function of only the chamber pressure

$$\frac{dm_e}{dt} = 17.23\ P_c \text{ in gm/sec} \qquad (20)$$

The mass within the chamber at any instant in time can be expressed by the equation of state

$$m_{CV} = P_c V/RT \qquad (21)$$

The rate of change in the mass can be determined by differentiating, that is:

$$\frac{dm_{CV}}{dt} = \frac{V}{RT}\frac{dP_c}{dt} \qquad (22)$$

or rearranging

$$\frac{dP_c}{dt} = \left(\frac{RT}{V}\right)\frac{dm_{CV}}{dt} \qquad \frac{RT}{V} \text{ is a constant} \qquad (23)$$

where:

$\frac{dP_c}{dt}$ = rate of pressure change, MPa/sec

$\frac{dm_{CV}}{dt}$ = rate of mass change, gm/sec

R = gas constant, 0.1103 gm-cal/gm-°K

T = 1042° K

V = internal volume of chamber, 8803 cm^3

therefore, after substitution of the known and constant term

$$\frac{dP_c}{dt} = 0.051\frac{dm_{CV}}{dt} \qquad (24)$$

therefore, substituting Equations 20 and 24 into Equation 16 and rearranging

$$\frac{dP_c}{dt} = .051(180 - 17.23\ P_c) \qquad (25)$$

Rearranging and integrating Equation 25 within the pressure limits of 0 to 5.88 MPa

$$\int_0^{5.88} \frac{dP_c}{(180 - 17.23P_c)} = \int_o^t 0.051\,dt \qquad (26)$$

$$t = 0.94 \text{ seconds}$$

Therefore, the flow into the test chamber is critical for one second. After this time, the ramps must initiated to open the valves further.

FLOW ANALYSIS OF THE WATER

The flowrate of the water can be controlled by several methods: via the flow control valve or by regulating the pump stroke rate. The water pump is a positive displacement type and thus discharges water in discrete volumes rather than as a continuous and uniform flow. Consequently, the pressure drop across the flow control valve varies cyclically and directly with the flowrate. This relationship can be expressed as:

$$Q = 1.44\ C_V\sqrt{\frac{\Delta P}{SG}} \qquad (27)$$

where:

Q = volumetric flowrate, l/min

C_V = flow coefficient of valve

ΔP = pressure drop across valve, KPa

SG = specific gravity, 1.0 for water.

The flow capacity curve for the water metering valve, as specified by the manufacturer is shown in Figure 31.

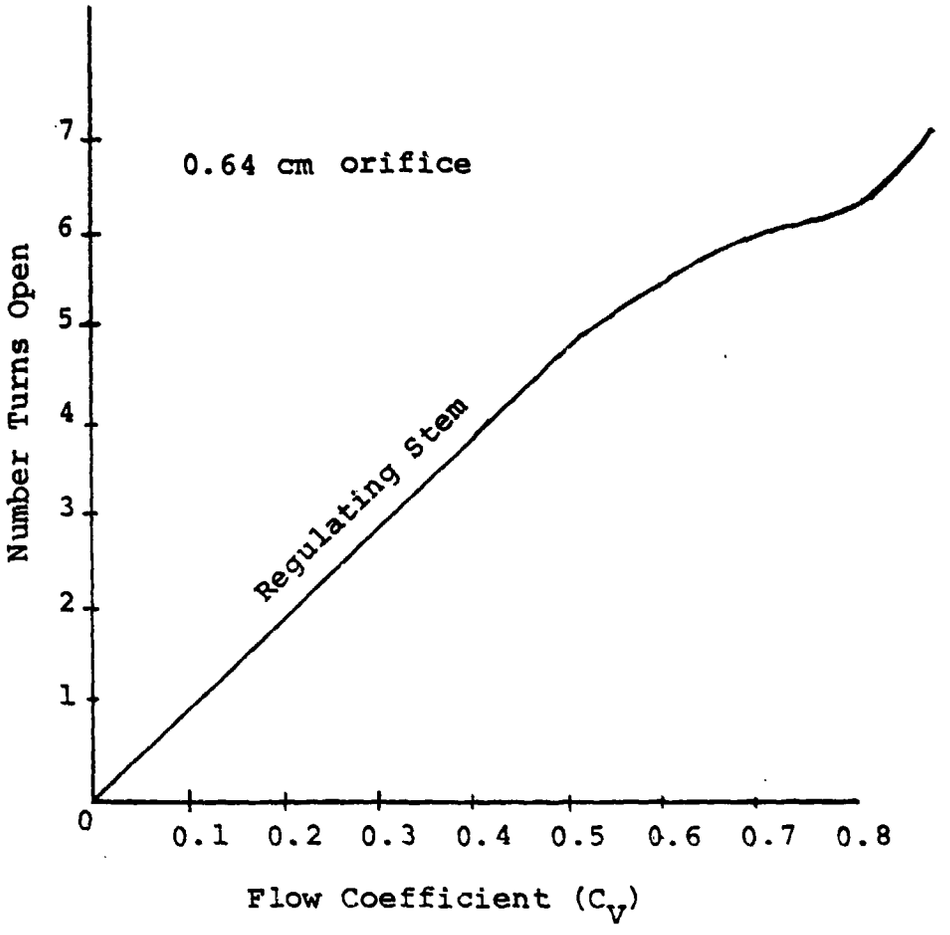

Figure 31. Flow capacity curve for the water valve.

The flow capacity curve is linear through most of its range. However, the flowrate cannot be accurately calculated based on a ΔP measurement which is cyclic. Therefore, water flow control is difficult with a metering valve.

A more accurate means of controlling the water flowrate is by regulating the stroke rate of a positive displacement pump. A discrete volume of water is discharged during each pump stroke. Since the pump stroke rate can be changed, via the air drive pressure and flowrate, it can be adjusted to provide any required water flowrate. In the steam generator

system, the stroke rate is monitored by sensing pressure cycles using a differential pressure transducer installed across the water valve. The stroke rate can thus be monitored from the strip chart recorder.

The discharge volume of 49 cm^3 per stroke was determined by accurately measuring the volume of water discharged during a 2-minute run and counting the number of strokes. The flowrate as a function of the stroke rate can be expressed as:

$$V = 2.94 \times S \qquad (28)$$

where:

V = volumetric flowrate, l/min
S = stroke rate, strokes/sec

VI. DATA AND RESULTS

Numerous experiments were performed utilizing the hydrogen-oxygen steam-generator. The data for two successful runs at high flowrates and temperature and pressures are presented in this report. Included in this section are the strip chart recordings of the pressure and temperatures of the steam generated as a function of time. Also experiment and instrumentation sheets are provided for each experiment. The experiment sheet contains the test parameters such as valve settings, steam and water orifice diameters and the pump stroke rate, as precalculated based upon the appropriate equations presented in this report. The instrumentation along with the chart span and chart speed for each channel of recording are tabulated in an instrumentation sheet. The experimental data are compared with theoretical calculations for correlation purposes and presented per experiment.

EXPERIMENT I (6/27/79)

For this experiment, critical flow of hydrogen and oxygen occurred throughout the entire run since the steam exit orifice was sized to maintain test chamber pressure at 3.28 MPa. Thus, the ratio $P_{chamber}/P_{reactant} < 0.528$. The steam pressure and temperatures recorded at the end of the 60-second run were 1.59 MPa with 199°C temperature at the bottom of the chamber and 188°C at the top. Both the temperature and pressure of the steam appear to have stabilized and are assumed to be the steady-state, steady-flow conditions for the parameters in this experiment. The sharp initial increase in temperature shown on the strip chart recordings is a result of the few-second delay in turning on the water until assurance of ignition.

The temperatures at the top and bottom of the chamber agree within 11°C which indicates that the water spray was effective in controlling the flame temperature. This uniformity of temperature within the chamber also is an indication of the quality of the steam. At a pressure of 1.59 MPa, the saturation temperature for steam is 200°C. The recorded temperatures were only slightly below this value and therefore in excellent agreement with the theoretical temperature.

The discrepancy in the theoretical and experimental pressure and temperature for the steam can be attributed to numerous causes including: heat loss through the thermal insulation, inaccuracies in setting of valves and measurement errors. The heat loss through the thermal insulation is not quantifiable. However, at the conclusion of the test, the chamber wall was hot to the touch, estimated at about 100°C. Also, for this experiment, the servo controllers for the H_2 and O_2 valves were not operational. The valves were set by hand. Consequently the position of the valves could not be adjusted to an accuracy of better than 1/16th of a turn.

The actual flowrates of hydrogen and oxygen can be checked from the bottle pressure decay as indicated by the pressure gauges. The subdivisions on the gauges are in 0.69 MPa increments and thus can be read to an accuracy of not better the 0.17 MPa. This provides only a rough check of the flowrates. Charles Law states that: $P_1V_1 = P_2V_2$ assuming an ideal gas at a constant temperature. From this relationship, the initial and final volumes of gas in a bottle can be determined. From these volumes the average flowrate can be derived. The flowrates based on the bottle decays were 1.6 gm/sec and 25.6 gm/sec respectively. This is a lean mixture. The flowrates should have been 2 gm/sec of H_2 and 16 gm/sec of O_2. Consequently, the adiabatic flame temperature will be lower.

In addition, the flowrate of the water is subject to error. There are several methods of checking the actual flowrate. The amount of water displaced from the water tank can be determined from the change in water level. This check gives a flow of 5.3 l/min. Based on the stroke rate of 0.86 cycles/sec, the flowrate was 5.1 l/min. The flowrate can also be determined from the pressure drop across the metering valve. For a ΔP of 0.25 MPa and a valve C_V of 0.2, the flowrate is 4.5 l/min. This is the least accurate check since the ΔP is not constant but cyclic. Also there are errors in setting the C_V for the valve. These results suggest that the flowrate for the water was high since 4.7 l/min is ideal.

For the case of 1.6 gm/sec of H_2 and 25.6 gm/sec of O_2 reacting with injection of 5.1 l/min of water, the heat of combustion is sufficient to vaporize only part of the water. Consequently, the steam pressure and temperature will be lower.

EXPERIMENT SHEET

Experiment No. I
Date 27 June 1979
Test Engr. L.D. Ellefson

1. PRESSURE REGULATOR SETTINGS:
   - Hydrogen hand reg. (HR-101) : 1300 PSIG
   - Oxygen hand reg. (HR-102) : 1300 PSIG
   - Nitrogen hand reg. (HR-103) : 1000 PSIG
   - Air regulator (HR-104) : 75 PSIG

2. METERING VALVE SETTINGS:
   - Hydrogen (ROV-101) : No. turns open .35 C_v .022
   - Oxygen (ROV-102) : No. turns open .70 C_v .043
   - Water (HV-106) : No. turns open 2 C_v .20
   - Air (HV-109) : No. turns open 1/2 C_v _____

3. FLOWRATES AND PRESSURES:
   - Hydrogen : 48 SCFM @ 1000 PSIG
   - Oxygen : 24 SCFM @ 1000 PSIG
   - Air : _____ SCFM @ 30 PSIG
   - Water : 1.25 GPM @ _____ PSIG

4. SUPPLY PRESSURES AND VOLUMES:
   - Hydrogen: Size/No.Bottles 1-K Pres. In/Fin 2150/1725 PSIG
   - Oxygen : Size/No.Bottles 1-T Pres. In/Fin 2500/2200 PSIG
   - Nitrogen: Size Bottle 1-T Pres. _____ PSIG
   - Water : Volume (Initial/Final) 10.6/9.2 GALS

5. STEAM EXIT ORIFICE DIAMETER: .21 INCHES

6. COMBUSTION CHAMBER TEMP. AND PRES. EXPECTED:
   - Temperature : 620 °F
   - Pressure : 460 PSIG

7. RUN TIME: 60 SECONDS

8. H_2O ORIFICE DIAMETER: .043 INCHES

9. PUMP STROKE RATE 8 Cycles/10 sec

REMARKS

1. Air Drive Pres, 30 PSI
2. Pump Discharge Pres., 1100 PSI

INSTRUMENTATION SHEET

Experiment No. I

Date 27 June 1979

Instrument Engr. D. Harrison

1. PRESSURE TRANSDUCERS

Channel No.	Location of Transducer	Diaphragm Size (PSIG)	Expected Pres. (PSIG)
P_1	Inlet H_2 Valve	2000	1000
P_2	Outlet H_2 Valve	2000	460 Max
P_3	Inlet O_2 Valve	2000	1000
P_4	Outlet O_2 Valve	2000	460 Max
P_5	Chamber	2000	460 Max
P_6	Across Water Valve	2000	40

2. TEMPERATURE TRANSDUCERS

Channel No.	Location of Transducer	Type of Thermocouple	Expected Max Temp (°F)
T_1	Bottom of Chamber	K	620
T_2	Top of Chamber	K	620

3. STRIP CHART RECORDERS

Channel No.	Data Temp/Pres.	Chart Speed (In/Min)	Chart Span (Full-Scale)
1 (P_5)	Pres	6	5 Volts
2 (T_2)	Temp	6	50 Millivolts
3 (T_1)	Temp	6	50 Millivolts
4 (P_5)	Pres	6	2 Volts
5 (P_2)	Pres	6	5 Volts
6 (P_4)	Pres	6	5 Volts
7 (P_1)	Pres	6	10 Volts
8 (P_3)	Pres	6	10 Volts

(Experiment I, 6/27/79)

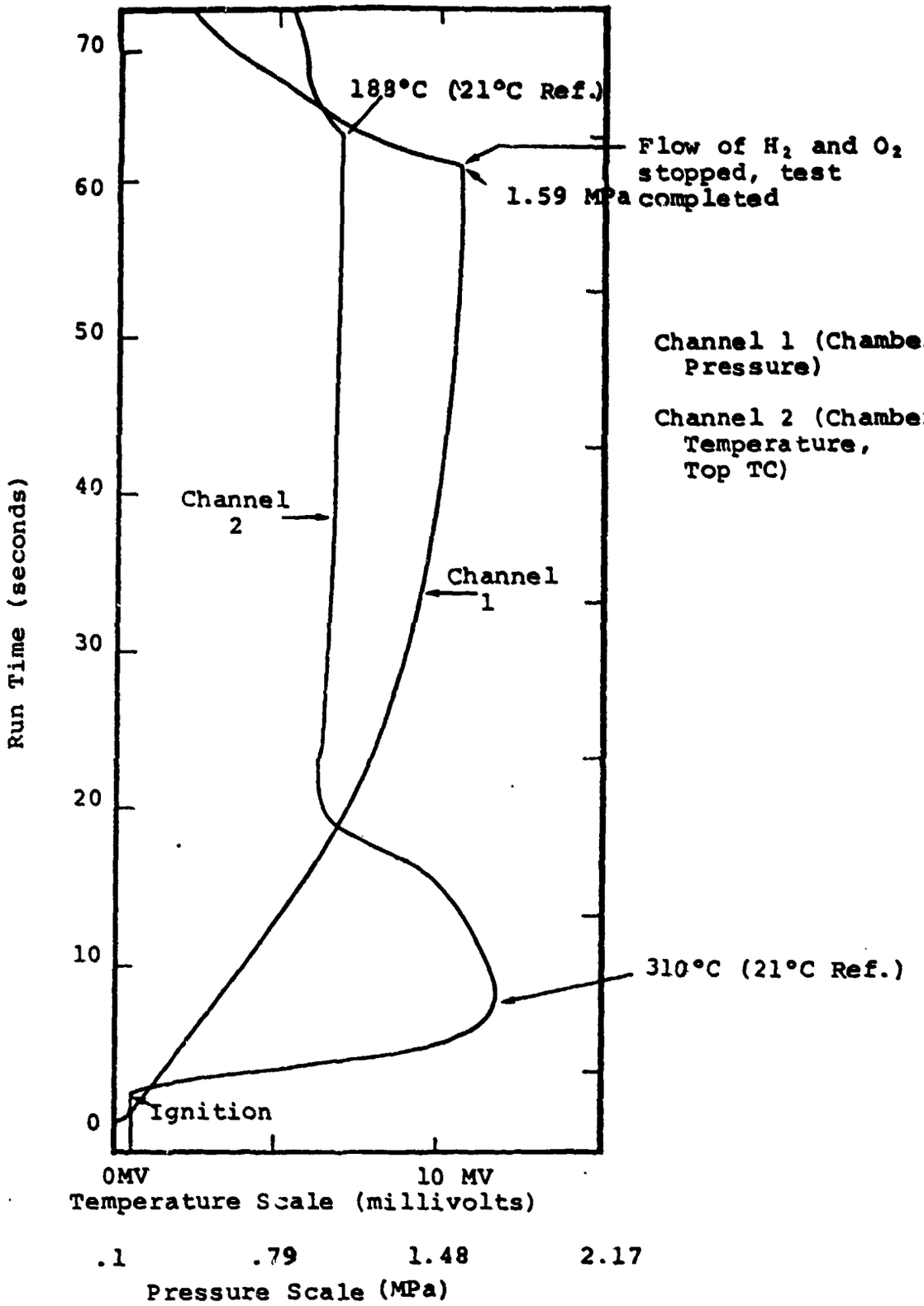

Figure 32. Strip chart recording of the chamber pressure and temperature.

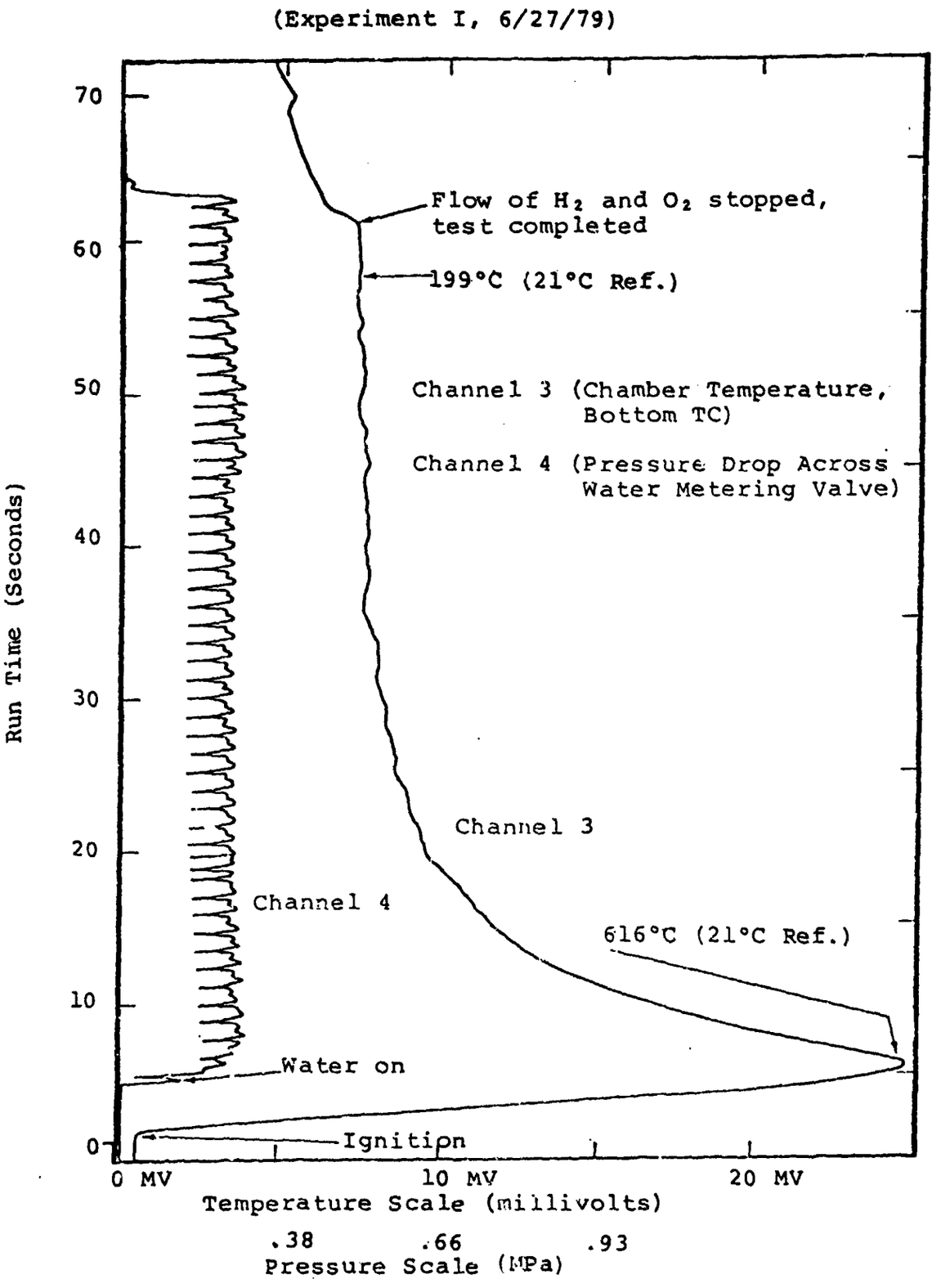

Figure 33. Strip chart recording of chamber temperature and ΔP across water metering valve.

EXPERIMENT II (6/29/79)

For this experiment, the flows of H_2 and O_2 were maintained critical. The metering valves were set by hand. The assumed steady-state, steady-flow conditions at the end of the 60-second run were 4.52 MPa with a 254°C temperature at the bottom of the chamber and a temperature of 243°C at the top. Here again the temperature gradient within the chamber was small, only 11°C. The recorded temperatures agreed closely with the saturation temperature of 257°C for steam at 4.52 MPa.

The flowrates of H_2 and O_2 based on the bottle pressure decay were 0.76 gm/sec and 21.6 gm/sec, respectively. These are lower than expected which results in a lower flame temperature. The water flowrate (based on a stroke rate of 0.83 cycles/sec) was 4.9 l/min. The flowrate based on ΔP across the metering valve, was 3.6 l/min. Thus the water flowrate seems slightly lower than the desired 5.3 l/min. However, for flows of 0.76 gm/sec of H_2 and 21.6 gm/sec of O_2 with injection of 4.9 l/min of water, the heat of combustion was sufficient to vaporize only part of the water. As a result, the expected temperature of 427°C and pressure of 9.34 MPa was not attained.

EXPERIMENT SHEET

Experiment No. II

Date 29 June 1979

Test Engr. L.D. Ellefson

1. PRESSURE REGULATOR SETTINGS:

Hydrogen hand reg. (HR-101) :	2000	PSIG
Oxygen hand reg. (HR-102) :	2000	PSIG
Nitrogen hand reg. (HR-103) :	1700	PSIG
Air regulator (HR-104) :	80 (75 flowing)	PSIG

2. METERING VALVE SETTINGS:

Hydrogen (ROV-101) : No. turns open	.26	C_v	.0166	
Oxygen (ROV-102) : No. turns open	.55	C_v	.033	
Water (HV-106) : No. turns open	2	C_v	0.2	
Air (HV-109) : No. turns open	1/2	C_v		

3. FLOWRATES AND PRESSURES:

Hydrogen :	60	SCFM @	1700	PSIG
Oxygen :	30	SCFM @	1700	PSIG
Air :		SCFM @	30	PSIG
Water :	1.4	GPM @		PSIG

4. SUPPLY PRESSURES AND VOLUMES:

Hydrogen: Size/No.Bottles 3-K Pres. In/Fin 2100/1900 PSIG

Oxygen : Size/No.Bottles 1-T Pres. In/Fin 2850/2600 PSIG

Nitrogen: Size Bottle 1-T Pres. PSIG

Water : Volume (Initial/Final) 11.0/ GALS

5. STEAM EXIT ORIFICE DIAMETER: .14 INCHES

6. COMBUSTION CHAMBER TEMP. AND PRES. EXPECTED:

Temperature : 800 °F

Pressure : 1340 PSIG

7. RUN TIME: 60 SECONDS

8. H_2O ORIFICE DIAMETER: .046 INCHES

9. PUMP STROKE RATE 9 Cycles/10 sec

REMARKS

1. Air Drive Pres, 30 PSIG
2. Pump Discharge Pres, 1150 PSIG
3. 304 S.S. Liner Installed

INSTRUMENTATION SHEET

Experiment No. II

Date 29 June 1979

Instrument Engr. Dan Harrison

1. PRESSURE TRANSDUCERS

Channel No.	Location of Transducer	Diaphragm Size (PSIG)	Expected Pres. (PSIG)
P_1	Inlet H_2 Valve	2000	1700
P_2	Outlet H_2 Valve	2000	1340 Max
P_3	Inlet O_2 Valve	2000	1700
P_4	Outlet O_2 Valve	2000	1340 Max
P_5	Chamber	2000	1340 Max
P_6	Across Water Valve	2000	50

2. TEMPERATURE TRANSDUCERS

Channel No.	Location of Transducer	Type of Thermocouple	Expected Max Temp (°F)
T_1	Bottom of Chamber	K	800
T_2	Top of Chamber	K	800

3. STRIP CHART RECORDERS

Channel No.	Data Temp/Pres.	Chart Speed (In/Min)	Chart Span (Full-Scale)
1 (P_5)	Pres	6	10 Volts
2 (T_2)	Temp	6	50 Millivolts
3 (T_1)	Temp	6	50 Millivolts
4 (P_6)	Pres	6	2 Volts
5 (P_2)	Pres	6	10 Volts
6 (P_4)	Pres	6	10 Volts
7 (P_1)	Pres	6	10 Volts
8 (P_3)	Pres	6	10 Volts

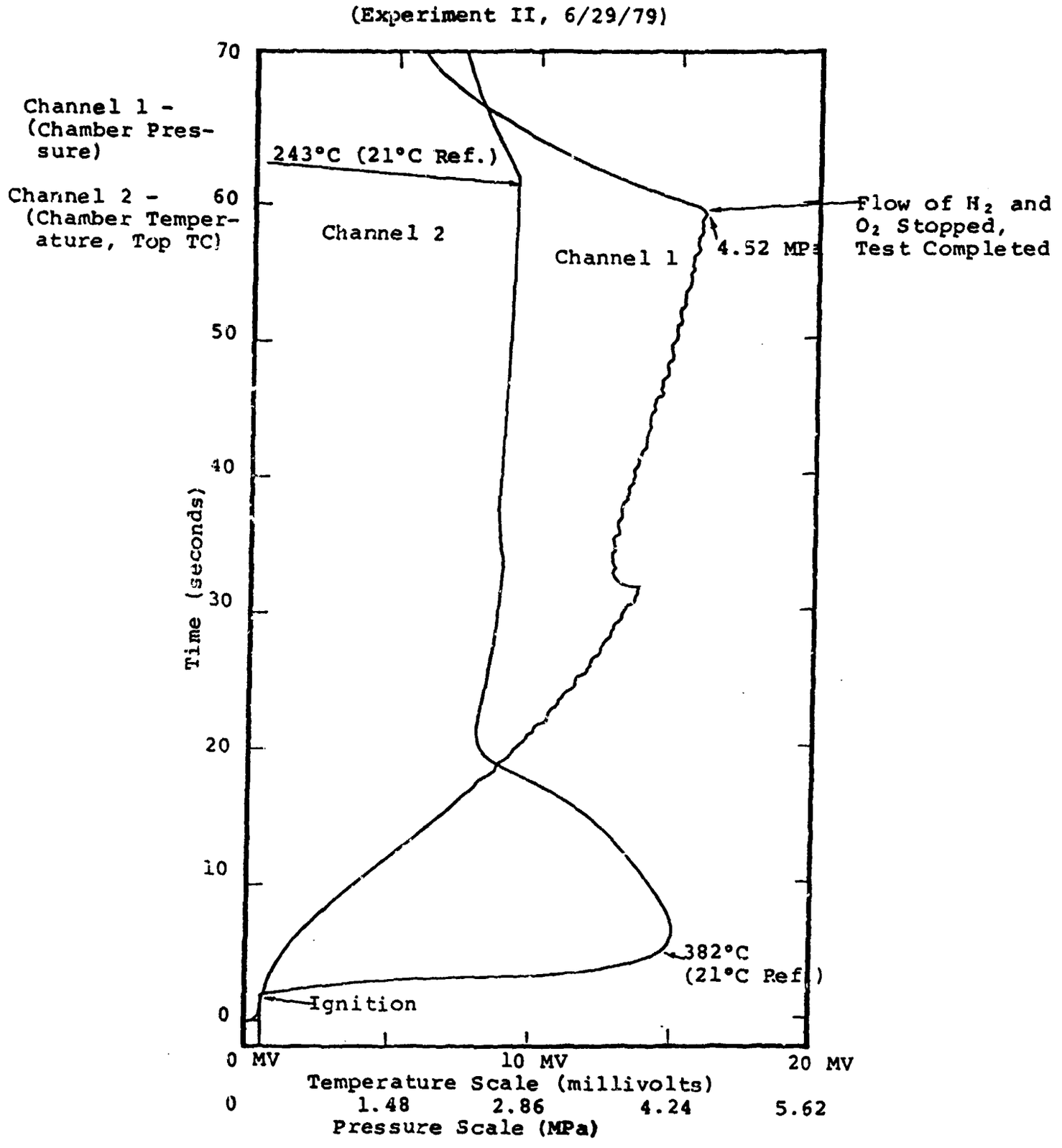

Figure 34. Strip chart recording of the chamber pressure and temperature.

(Experiment II, 6/29/79)

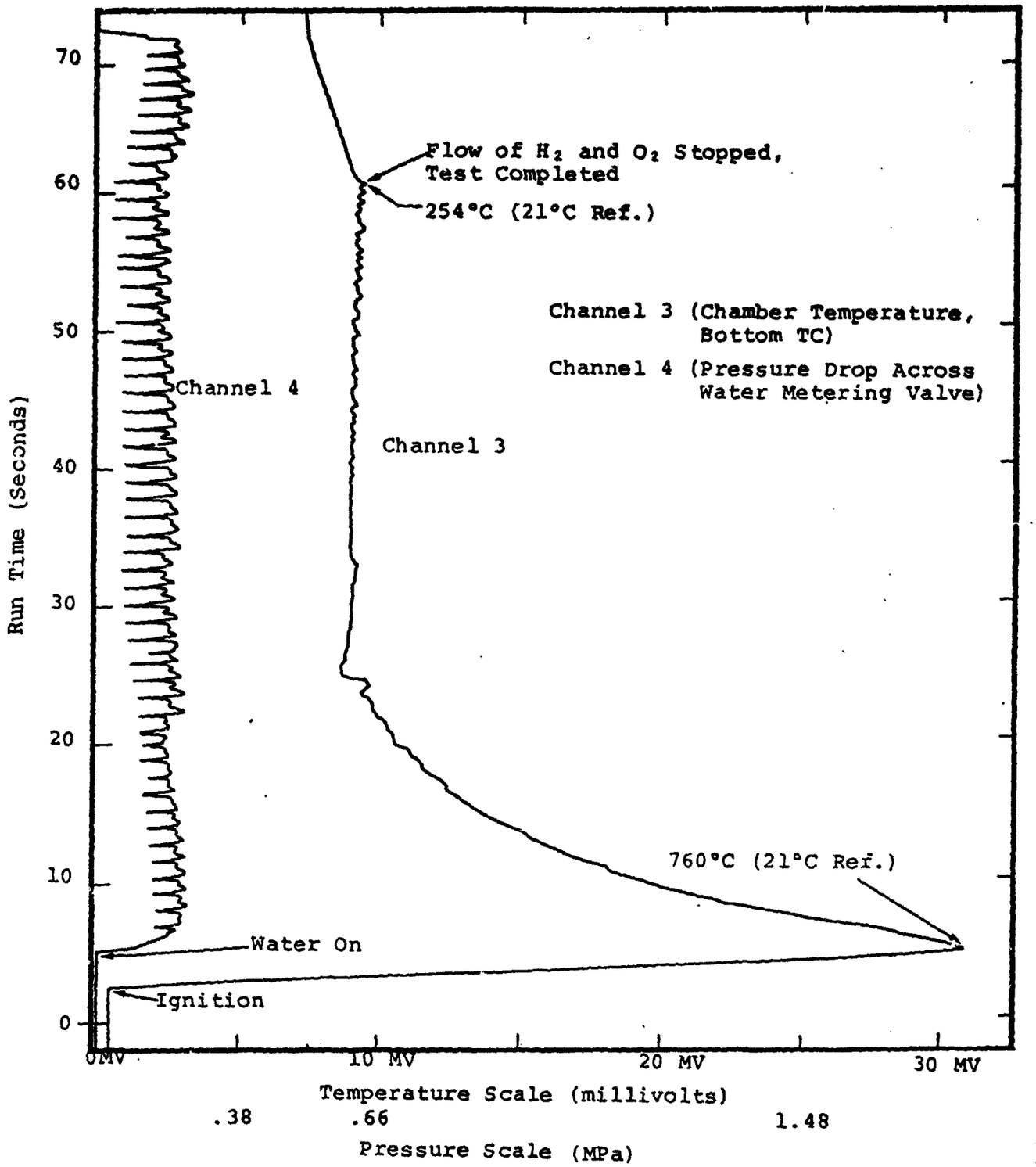

Figure 35. Strip chart recording of the chamber temperature and ΔP across water valve.

APPENDIX A

CALCULATION OF THE ADIABATIC FLAME TEMPERATURE

Calculation of the adiabatic flame temperature for the chemical reaction of two moles of hydrogen and one mole of oxygen with the addition of six (n=6) moles of water is as follows. This reaction can be expressed as:

$$2\ H_2 + O_2 + 6\ H_2O \rightarrow 8\ H_2O \qquad \text{(A-1)}$$

The first law of thermodynamics for a steady-state, steady flow process expressed as a rate equation is:

$$\dot{Q}_{CV} + \dot{m}_i\left(h_i + \frac{V_i^2}{2g_c} + z_i\frac{g}{g_c}\right) = \dot{W}_{CV} + \dot{m}_e\left(h_e + \frac{V_e^2}{2g_c} + z_e\frac{g}{g_c}\right) \qquad \text{(A-2)}$$

Where:

$\dot{Q}_{CV}$ = Rate of heat transfer across the system boundary

$\dot{W}_{CV}$ = Rate of work crossing the system boundary

$\dot{m}_i$, $\dot{m}_e$ = Mass flowrates in and out of the control volume

h_i, h_e = Enthalpy of the constituents entering and leaving the control volume per unit mass.

$\frac{V_i^2}{2g_c}$, $\frac{V_e^2}{2g_c}$ = Kinetic energy of the constituents entering and leaving the control volume per unit mass.

$z_i\frac{g}{g_c}$, $z_e\frac{g}{g_c}$ = Potential energy of the constituents entering and leaving the control volume per unit mass.

For a combustion process, the changes in the kinetic and potential energies are negligible. Also the process is adiabatic and no work crosses the system boundary. Therefore, these terms can be eliminated from the expression, thus, the enthalpy of the reactants equals the enthalpy of the product.

$$\dot{m}_i h_i = \dot{m}_e h_e \qquad \text{(A-3)}$$

or

$$\sum_{R} n_i \left[\bar{h}_f^\circ + (\bar{h} - \bar{h}_{298}^\circ) \right]_i = \sum_{P} n_e \left[\bar{h}_f^\circ + (\bar{h} - \bar{h}_{298}^\circ) \right]_e \qquad \text{(A-4)}$$

Where:

n_i, n_e = Number of moles entering and leaving, respectively

$\bar{h}_f^\circ$ = Enthalpy of formation of a compound at 25°C and 0.1 MPa with reference to the enthalpy of its elements which are assumed to be equal to zero at 25°C and 0.1 MPa.

$(\bar{h} - \bar{h}_{298}^\circ)$ = Enthalpy at a given thermodynamic state minus the enthalpy at 25°C and 0.1 MPa.

Assuming the reactants enter at 25°C and that H_2, O_2, and H_2O are ideal gases and therefore their enthalpies are independent of pressure, the $(\bar{h} - \bar{h}_{298}^\circ)$ terms for the reactants reduce to zero. Also the enthalpy of formation of H_2 and O_2 are zero since they are not compounds but elements.

Thus equation A-4 reduces to

$$n_i \bar{h}_f^\circ)_{H_2O\ (\ell)} = n_e \left[\bar{h}_f^\circ + (\bar{h} - \bar{h}_{298}^\circ) \right]_{H_2O(g)} \qquad \text{(A-5)}$$

The enthalpy of formation for water in the liquid state at 25°C and 0.1 MPa is -68,317. The negative sign indicates that heat is liberated when water is formed. The heat of formation of water in the gaseous state at 25°C and 0.1 MPa is equal to -57,798 cal/gm-mole.

Therefore, after substituting known values, equation A-5 reduces to:

$$6(-68,317) = 8(-57,798) + 8(\bar{h} - \bar{h}_{298}^\circ) \qquad \text{(A-6)}$$

Reducing and rearranging:

$$(\bar{h} - \bar{h}_{298}^\circ) = 6560$$

This increase in enthalpy of steam of 6560 cal/gm-mole corresponds to a temperature of 769°C, as determined from the thermodynamic tables for the heat of formation of water.

APPENDIX B
CALIBRATION OF FLOW CONTROL VALVES

The hydrogen and oxygen servo-controlled metering valves were calibrated using air to obtain the flow capacity curves (flow coefficient, C_v, versus the number of turns open). These curves for the H_2 and O_2 valves are shown in Figures B-2 and B-3 respectively. Notice that they are both roughly linear throughout the full range of the valves (from zero to seven turns maximum). The slight variation in the two curves may be the result of minor differences in the machining and assembly tolerance of the valves.

Actual calibration of the valves was performed via a flow test bench designed and built by Systems, Science and Software. The test set-up is shown in Figure B- below.

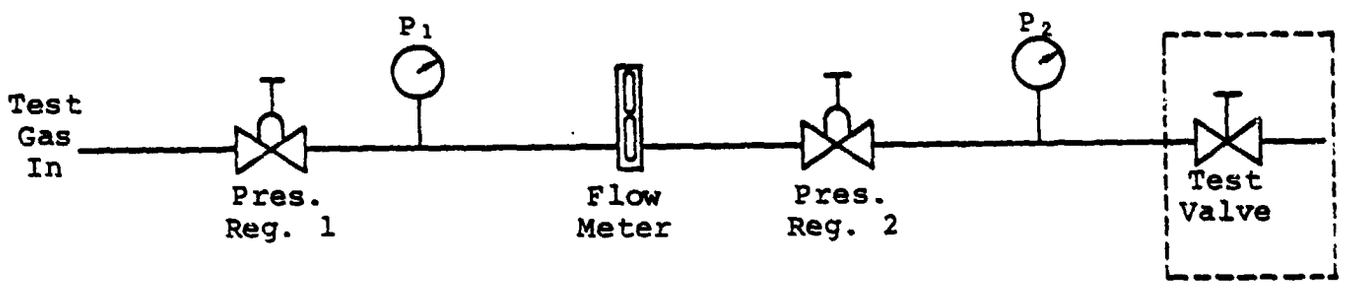

Figure B-1. Calibration of a valve.

The test medium was air at 22°C, regulated to 0.45 MPa. The pressure upstream of the flowmeter, P_1, and the pressure upstream of the test valve, P_2, were maintained constant at 0.45 MPa and 0.24 MPa respectively by adjusting the pressure regulators for each valve setting. Thus the flow through the

test valves was maintained critical at all times, that is, $P_{atm}/P_2 < 0.528$. Therefore, the flow coefficient at each valve setting can be calculated using the critical flow equation:

$$C_V = \frac{Q_G}{694\ P_2}\sqrt{SG \times T} \qquad \text{(B-1)}$$

$$Q_G = Q_A\sqrt{\frac{P_1}{0.1} \times \frac{294}{T}} \qquad \text{(B-2)}$$

where:

Q_A - actual gas flowrate read from flowmeter converted to l/sec

Q_G - gas flowrate corrected for temperature and pressure (l/sec @ STP)

S_G - specific gravity of gas, 1.0 for air

T - temperature of gas (°K)

P_1 - inlet pressure to flowmeter (MPa)

P_2 - inlet pressure to test valve (MPa)

C_V - flow coefficient of valve

The test data for the two valves are shown in Tables B-1 and B-2.

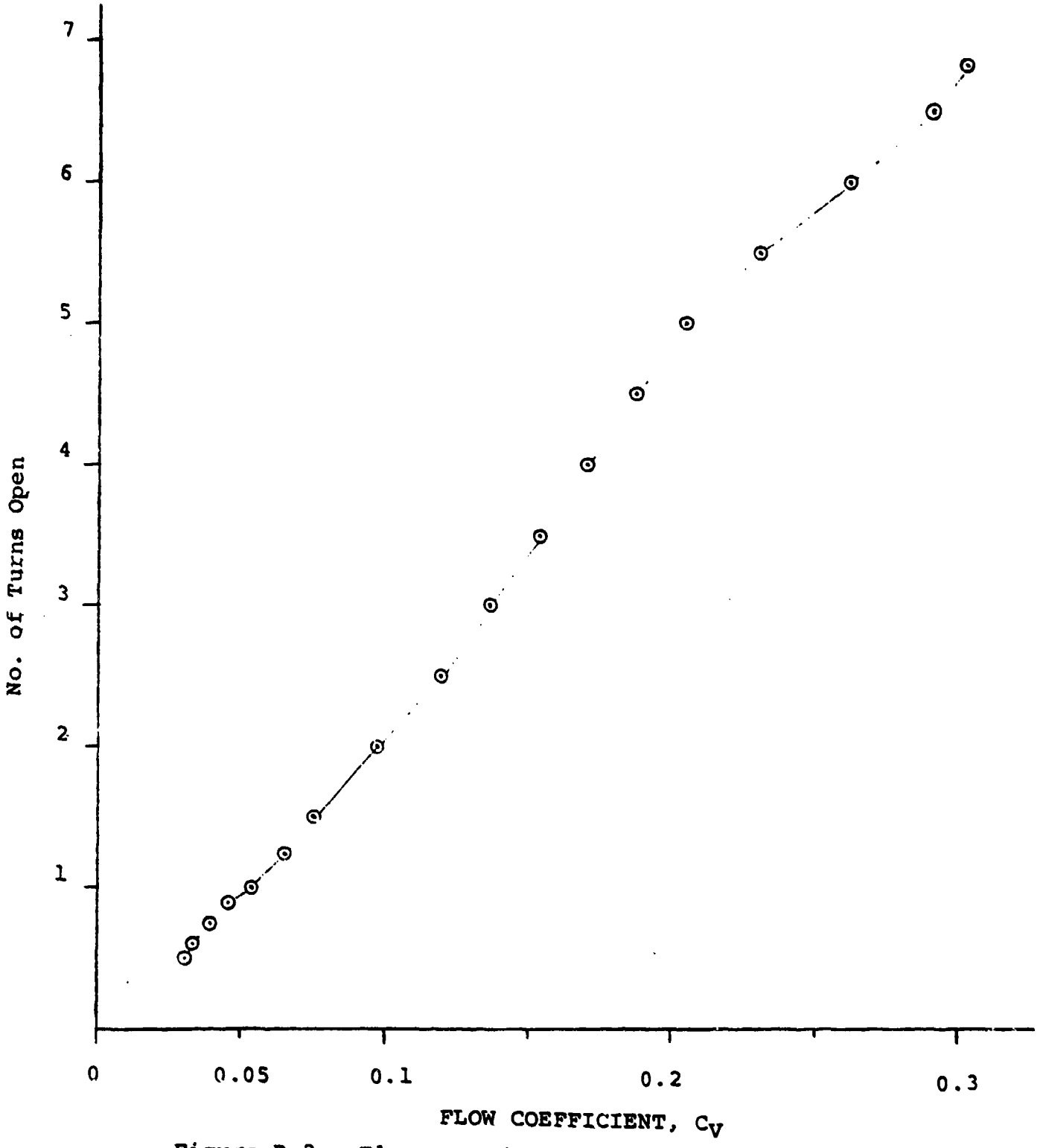

Figure B-2. Flow capacity curve for the H_2 valve.

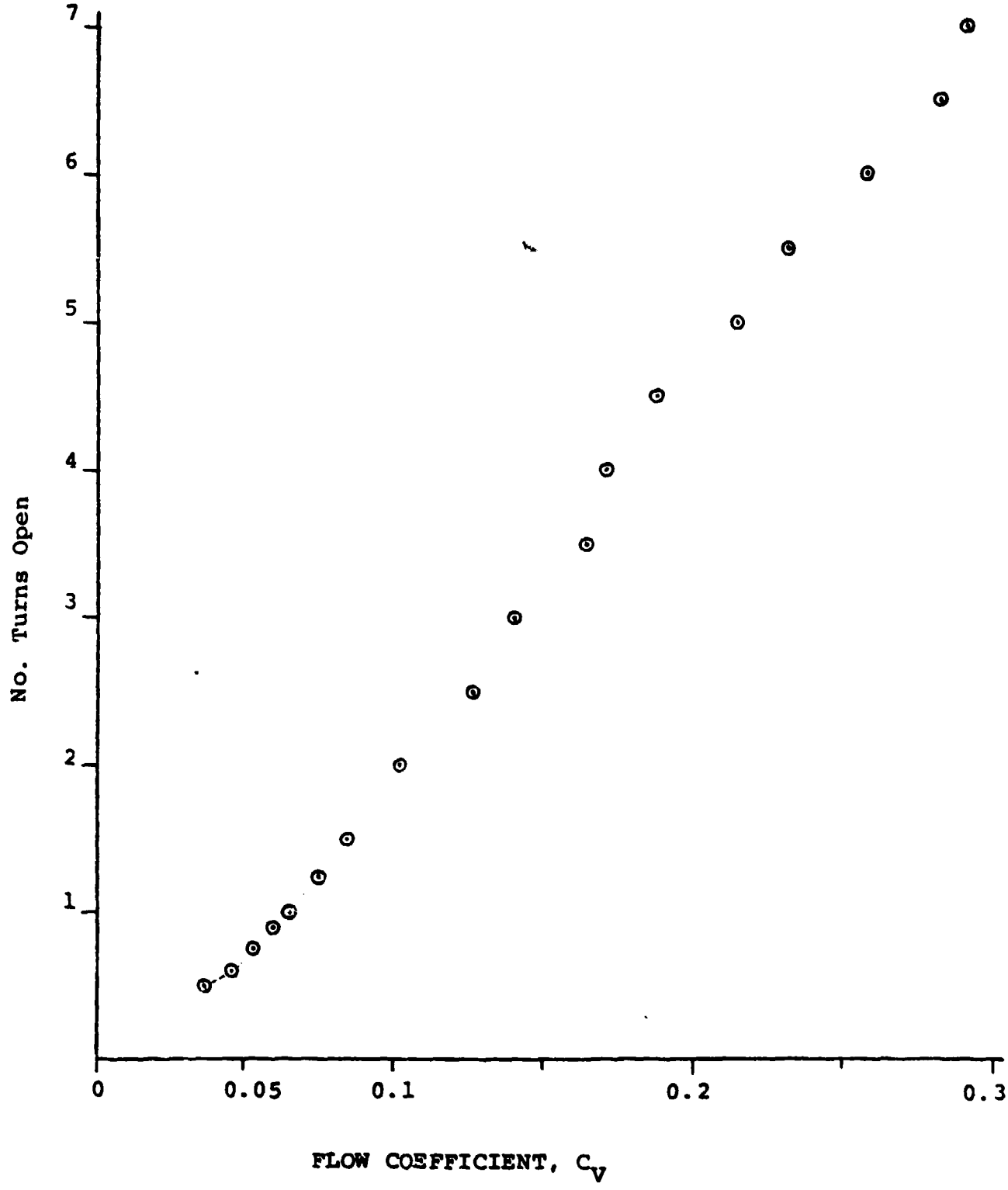

Figure B-3. Flow capacity curve for the O_2 valve.

TABLE B-1

TEST DATA FOR THE H_2 VALVE

P_1 (MPa)	P_2 (MPa)	Q_A (ℓ/sec)	No. Turns Open	C_V
0.45	0.24	0.145	0.5	0.031
0.45	0.24	0.157	0.6	0.034
0.45	0.24	0.185	0.75	0.040
0.45	0.24	0.212	0.9	0.046
0.45	0.24	0.252	1.0	0.054
0.45	0.24	0.299	1.25	0.065
0.45	0.24	0.346	1.5	0.075
0.45	0.24	0.448	2.0	0.097
0.45	0.24	0.551	2.5	0.119
0.45	0.24	0.629	3.0	0.136
0.45	0.24	0.708	3.5	0.153
0.45	0.24	0.787	4.0	0.170
0.45	0.24	0.865	4.5	0.187
0.45	0.24	0.944	5.0	0.204
0.45	0.24	1.06	5.5	0.230
0.45	0.24	1.20	6.0	0.261
0.45	0.24	1.34	6.5	0.290
0.45	0.24	1.39	6.8	0.302

TABLE B-2

TEST DATA FOR THE O_2 VALVE

P_1 (MPa)	P_2 (MPa)	Q_A (ℓ/sec)	No. Turns Open	C_V
0.45	0.24	0.173	0.5	0.037
0.45	0.24	0.212	0.6	0.046
0.45	0.24	0.244	0.75	0.053
0.45	0.24	0.275	0.9	0.060
0.45	0.24	0.299	1.0	0.065
0.45	0.24	0.346	1.25	0.075
0.45	0.24	0.393	1.5	0.085
0.45	0.24	0.472	2.0	0.102
0.45	0.24	0.582	2.5	0.126
0.45	0.24	0.645	3.0	0.140
0.45	0.24	0.755	3.5	0.164
0.45	0.24	0.787	4.0	0.170
0.45	0.24	0.865	4.5	0.187
0.45	0.24	0.983	5.0	0.213
0.45	0.24	1.06	5.5	0.230
0.45	0.24	1.18	6.0	0.256
0.45	0.24	1.30	6.5	0.281
0.45	0.24	1.34	7.0	0.290

APPENDIX C

SPECIFICATIONS FOR THE THERMAL INSULATION

The thermal insulation is made from layers of woven silica/alumina manufactured by the Carborundum Corporation. The top and bottom plates are Fiberfrax Duraboard, a rigid, high temperature board made from bulk ceramic fibers and inorganic bonding agents. The cylindrical sleeve is layers of Fiberfrax Durablanket, a strong flexible blanket made from long ceramic fibers, cross-locked for high handling strength. For a 5.08 cm-thickness of Duraboard and Durablanket insulation, the cold face temperature will be 127°C based on a hot face temperature of 815°C. The physical properties of the insulation are shown in Table C-1.

TABLE C-1

PHYSICAL PROPERTIES OF THE THERMAL INSULATION*

	Durablanket	Duraboard
Density, gm/cm^3	0.13	0.48
Thermal conductivity, $cal/sec\text{-}cm^2\text{-}°C/cm$	4.5×10^{-4} (@ 815°C)	4.1×10^{-4} (@ 815°C)
Specific heat, cal/gm-°C	0.27 (@ 1090°C)	--
Continuous use limit	1260°C	1260°C

* Data courtesy of Aerospex Corporation, a registered distributor of Carborundum Corporation.

APPENDIX D

SAFETY AND SYSTEM CHECK OUT

CLEANLINESS

The hydrogen and oxygen lines, and especially the oxygen lines, must be maintained very clean. In the case of oxygen, it is known that disastrous fires have occurred due to the tightening of a threaded joint on an insect. Allowing oxygen to flow across this slightly heated up organic matter was sufficient to encourage combustion. The hydrogen and oxygen fluid transfer lines and associated valving were cleaned for gaseous oxygen service both before and after installation. Also elaborate procedures were taken to ensure that the systems, and in particular the flow metering valves and pressure regulators, were maintained in a clean condition. In addition, the dome pressure regulators as well as the metering valves for both the H_2 and O_2 were "LOX" cleaned by certified laboratories. After complete assembly, both systems were flushed with tricloroethylene to remove any hydrocarbons or loose debris, followed by immediate drying by purging with dry nitrogen. The compatibility of all materials, including seals, was investigated to prevent possible undesirable reactions with H_2 or O_2. Only teflon tape and/or liquid teflon pipe sealant, both compatible with oxygen, were used on threaded connections.

LEAK AND PROOF PRESSURE TESTING

The Chamber and fluid transfer lines (O_2, H_2 and H_2O) were proof and leak pressure tested as a system to 11.8 MPa for 30 minutes using nitrogen. All connections were flushed with a soap bubble solution (SNOOP) to detect possible leaks. Also prior to a run, a leak test using nitrogen at 10.45 MPa was performed on the system to test the integrity of recently made-up connections. In addition, hydrogen heats up upon expansion at normal temperatures due to the reverse Joule-Thompson effect. Thus, an escaping stream of gas from a high

pressure line could conceivably reach the ignition temperature and ignite spontaneously. Extreme attention to detail in terms of cleanliness and prevention of catastrophic leaks is essential to the safe operation of a system such as described within this report.

FUNCTIONAL CHECK-OUT

The torch was dry run using nitrogen to simulate the flow of hydrogen and oxygen. This allowed the experimenters to become confident with the operation and control of the torch while in a safe mode. The torch was dry run at various combinations of both high and low pressures and flowrates so as to provide a thorough functional test for all equipment and instrumentation. The torch was fired in the open air, chamber removed, to access the ease of controllability of the hydrogen, oxygen and water flow control valves. This also showed the effect of the flame turbulence upon the water spray pattern.

The torch was inserted into the test chamber and a series of flow/pressure experiments were undertaken to develop a "feel" for the operation of the torch under low pressure and low flowrate conditions.

Safety in operation of the torch was assured by strict adherence to written start-up and shut-down procedures. In addition, shot sheets containing all the proper flow control valve and pressure regulator settings were used for each run.

DISTRIBUTION LIST

DEPARTMENT OF DEFENSE

Defense Nuclear Agency
ATTN: SPTD, T. Kennedy
4 cy ATTN: TITL

Field Command
Defense Nuclear Agency
ATTN: FCTMD, W. Summa
ATTN: FCTK, C. Keller

Field Command Test Directorate
Defense Nuclear Agency
ATTN: FCTC, J. LaComb

Defense Technical Information Center
12 cy ATTN: DD

DEPARTMENT OF ENERGY

Department of Energy
Nevada Operations Office
ATTN: R. Newman

DEPARTMENT OF ENERGY CONTRACTORS

Lawrence Livermore National Laboratory
ATTN: D. Oakley
ATTN: B. Hudson
ATTN: B. Terhune
ATTN: J. Shearer

Los Alamos Scientific National Laboratory
ATTN: R. Brownlee
ATTN: E. Jones
ATTN: F. App
ATTN: A. Davis
ATTN: L. Germain

DEPARTMENT OF ENERGY CONTRACTORS (Continued)

Sandia National Laboratories
ATTN: C. Mehl
ATTN: C. Smith
ATTN: A. Bass

OTHER GOVERNMENT AGENCY

Department of the Interior
U.S. Geological Survey
ATTN: R. Carroll

DEPARTMENT OF DEFENSE CONTRACTORS

General Electric Company—TEMPO
ATTN: DASIAC

Pacifica Technology
ATTN: G. Kent

Physics International Co.
ATTN: E. Moore

SRI International
ATTN: A. Florence

Systems, Science & Software, Inc.
ATTN: R. Duff

Terra Tek, Inc.
ATTN: S. Green